Journal of Medicinal Chemistry

Article

pubs.acs.org/jmc

Discovery of Potent and Selective RSK Inhibitors as Biological Probes

Rama Jain,[†] Michelle Mathur,[†] Jiong Lan, Abran Costales, Gordana Atallah, Savithri Ramurthy, Sharadha Subramanian, Lina Setti, Paul Feucht, Bob Warne, Laura Doyle, Stephen Basham, Anne B. Jefferson, Mika Lindvall, Brent A. Appleton, and Cynthia M. Shafer*

Global Discovery Chemistry/Oncology & Exploratory Chemistry, Novartis Institutes for Biomedical Research, 5300 Chiron Way, Emeryville, California 94608, United States

Supporting Information

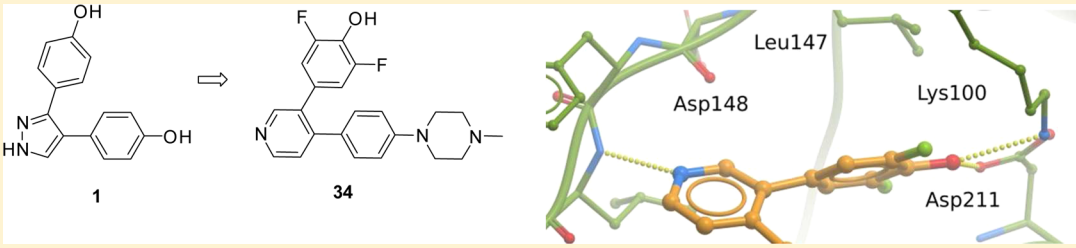

ABSTRACT: While the p90 ribosomal S6 kinase (RSK) family has been implicated in multiple tumor cell functions, the full understanding of this kinase family has been restricted by the lack of highly selective inhibitors. A bis-phenol pyrazole was identified from high-throughput screening as an inhibitor of the N-terminal kinase of RSK2. Structure-based drug design using crystallography, conformational analysis, and scaffold morphing resulted in highly optimized difluorophenol pyridine inhibitors of the RSK kinase family as demonstrated cellularly by the inhibition of YB1 phosphorylation. These compounds provide for the first time *in vitro* tools with an improved selectivity and potency profile to examine the importance of RSK signaling in cancer cells and to fully evaluate RSK as a therapeutic target.

INTRODUCTION

The p90 ribosomal S6 kinases (RSK) are a family of four serine/threonine kinases widely expressed across tissues and described to phosphorylate a number of proteins associated with functions as diverse as proliferation, apoptosis, motility, transcription, and EMT (epithelial-mesenchymal transition).[1−9] RSK kinases have an unusual structure in which an N-terminal kinase responsible for the phosphorylation of RSK's described substrates is fused to a C-terminal kinase that seems to be dedicated to activating the N-terminal RSK kinase. The current understanding of the activation scheme suggests that ERK (MAPK) phosphorylates and activates the C-terminal kinase, which then creates a phosphorylated docking site for PDK1 to bind to and activate the N-terminal kinase. This activation scheme has been accepted as canonical, but additional activating phosphorylation events have been described and may transfer the strict control of RSK activity from the MAP kinase signaling pathway to other signaling pathways.[1,2]

Though RSK undoubtedly phosphorylates its described substrates in model cell lines, it is unclear for which of these substrates and in which signaling contexts RSK phosphorylation is essential for substrate function. Complicating our understanding of RSK substrate phosphorylation in different cancer mutation contexts are the caveats of the tools available to inhibit the RSK isoforms. The four RSK isoforms are closely related, widely expressed, and likely to be at least somewhat redundant in their substrate phosphorylation. Thus, strong functional effects with traditional si/shRNAs targeting a single isoform are suspect. Chemical inhibitors of RSK isoforms also suffer from shortcomings, either because they target only a subset of the isoforms or because they inhibit additional kinases in addition to RSK.[10−12] As an example, BI-D1870[13] potently inhibits other kinases such as PLK1, which limits its utility in identifying cell lines sensitive to RSK. Further, a recent publication suggests that much of the cell signaling effects attributed to BI-D1870 are due to nonspecific effects.[14] The irreversible C-terminal kinase domain RSK inhibitor FMK,[15] however, is very selective but is not a pan-RSK inhibitor as RSK3 lacks the cysteine side-chain found in RSK1, 2, and 4 that is required to form the covalent adduct with FMK. Because it does not inhibit the RSK3 isoform, there was concern that RSK3 activity would be able to rescue phosphorylation events and functions that are shared among the four RSK isoforms. While FMK potently inhibits the phosphorylation of its substrate YB1, it fails to reach complete inhibition, suggesting that the residual activity is due to RSK3.[15] To address these limitations, an improved in vitro tool compound with good potency on all four RSK isoforms and improved selectivity was desired.

In an effort to identify new chemical starting points for identifying an improved tool molecule, a high-throughput screen (HTS) was carried out, which yielded a variety of scaffolds including bis-phenolpyrazole (**1**, Figure 1) as N-terminal kinase domain inhibitors of RSK2. Compound **1** was an attractive hit

Received: March 19, 2015

DOI: 10.1021/acs.jmedchem.5b00450
J. Med. Chem. XXXX, XXX, XXX−XXX

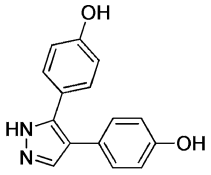

1

LE	0.54
RSK2	0.02 μM
pYB-1 TM	2.8 μM

Figure 1. RSK2 HTS pyrazole hit.

due to its high ligand efficiency (0.54) and its excellent selectivity against a panel of 69 kinases. These features suggested that it would be a good starting point to improve potency while maintaining selectivity. Although phenol moieties would be a concern in a typical medicinal chemistry hit-to-lead effort because they typically exhibit poor metabolic stability which translates to poor in vivo half-life, the goal of this effort was to develop an in vitro tool compound which diminished these concerns. Because **1** was a singleton hit in our screening deck, we began by verifying the chemical integrity of the hit by synthesizing several close analogues. These compounds exhibited similar biochemical potencies and assisted in confirming **1** as an excellent starting point for tool compound development to aid in the investigation of RSK biology in an oncologic setting. During the course of this work, the pyrazole series was morphed into a related 3,4-biaryl pyridyl series exemplified by **2** (Figure 2). Herein, we describe the hit

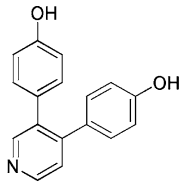

2

RSK2	0.18 μM
pYB-1 TM	9.3 μM

Figure 2. RSK2 pyridine analogue of **1**.

expansion of **1** and the hit-to-lead optimization of the 3,4-biaryl pyridyl series. This effort led to compounds **46** and **47**, which are highly selective and potent pan-RSK inhibitors that directly inhibit the phosphorylation of YB1 by RSK and inhibit cell growth in anchorage-independent settings. Compounds **46** and **47** were recently reported as LJH685 and LJI308, respectively, as biological probes for the elucidation of RSK signaling in cells.[16]

CHEMISTRY

The pyrazole analogues were synthesized by a Suzuki-Miyaura coupling[17] of **3** and **4** followed by bromination of the pyrazole C4 carbon with NBS (Scheme 1). A second Suzuki-Miyaura coupling gave the desired analogues (**1**, **26**–**29**). For the second Suzuki-Miyaura reaction, $PdCl_2$(dppf)·DCM was not an efficient catalyst for this system, and bis(di-*tert*-butylphosphino)ferrocene dichloropalladium(II) [$PdCl_2$(dtbpf)] was found to be consistently successful for this transformation.

The pyridine series was synthesized in one of two ways (Scheme 2). In the first route (Scheme 2, route 1), two

Scheme 1. General Synthesis of Pyrazole Analogues[a]

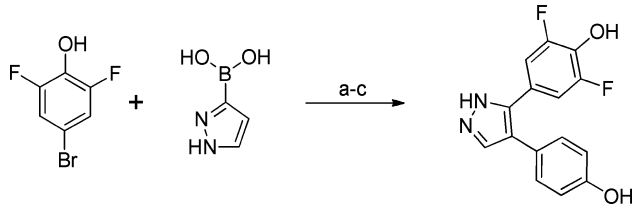

3 4 29

[a](a) 10% $PdCl_2$(dppf)·DCM, 2 M Na_2CO_3, DME, MW, 120 °C; (b) NBS, DMF, rt; (c) $ArB(OH)_2$, 10% $PdCl_2$(dtbpf), 2 M Na_2CO_3, DME, MW, 120 °C.

consecutive Suzuki-Miyaura couplings yielded the majority of the desired pyridine analogues (**30**–**49**). Depending on the availability of starting materials, some compounds were synthesized via an alternate route (Scheme 2, route 2) where the order of the Suzuki-Miyaura couplings were reversed beginning with an aryl (or heteroaryl) boronic acid (**7**) and 3-chloro-4-bromopyridine (**8**).

General schemes for the synthesis of 2-aminopyridine analogues are depicted in Scheme 3. For aliphatic amine substitued pyridines (Scheme 3, route 1), synthesis began with 2-fluoro-4-bromopyridine (**11**) which undergoes a Suzuki reaction, followed by S_NAr with a corresponding amine and bromination to provide the intermediate (**13**). Compound **13** was then reacted with a boronic ester (**14a** or **14b**) to provide final compounds (**51**–**52**). For **50**, the phenol was protected with a methyl group, but generally, the Suzuki reaction would proceed without the protection of the phenol. For aromatic amino-substituted pyridines (Scheme 3, route 2), the compounds were synthesized by carrying out the Suzuki coupling of 2-chloro-4-(4,4,5,5-tetramethyl-1,3,2-dioxaborolan-2-yl)-pyridine (**16**) with the aryl bromide (**17**) followed by a Buchwald reaction to furnish intermediate (**18**). After bromination and a final Suzuki coupling, **53** was produced.

Scheme 4 shows the two methods for the synthesis of the 2-aminopyrimidine series. Synthesis of **56** and **57** was achieved starting with 2,4-dichloropyrimidine (**19**). A Suzuki reaction followed by S_NAr and bromination to provide intermediate **21** and a final Suzuki coupling provided the desired products (Scheme 4, route 1). In the aminopyridmidine series, the S_NAr reaction proceeded smoothly, which enabled us to avoid the Buchwald reaction. The Buchwald reaction, however, was required to install the amine in the aminopyridine series.

The synthesis of **54** (Scheme 4, route 2) began with 4-chloropyrimidin-2-amine (**22**), thus eliminating the S_NAr reaction. Compound **22** was brominated and then coupled with **14a** to give **23**. The first Suzuki reaction to give **23** proceeded selectively at the 5-position, and the second Suzuki reaction proceeding at the 4 position to give **54**.

RESULTS AND DISCUSSION

Crystal Structure of RSK2 with Compound 1. The cocrystal structure of compound **1** in complex with the N-terminal kinase domain of RSK2 (Figure 3) was determined to gain structural insights into key pharmacophores and to guide our chemistry design activities. Compound **1** binds in the ATP pocket in a nonplanar, propeller-shaped conformation with one phenol projected toward the gatekeeper Leu147 and the second phenol projected under the P-loop. The pyrazole makes two

DOI: 10.1021/acs.jmedchem.5b00450
J. Med. Chem. XXXX, XXX, XXX−XXX

Scheme 2. General Syntheses for the Pyridine Series[a]

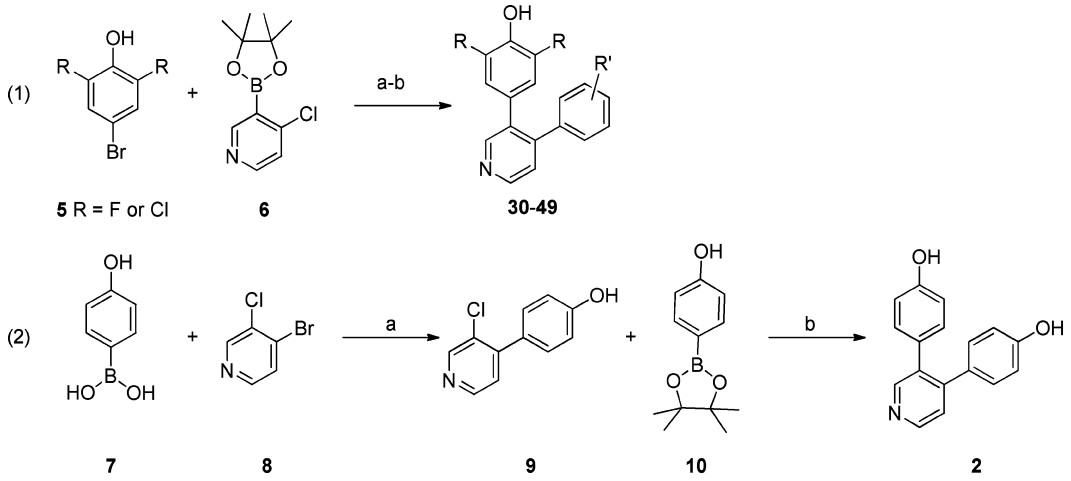

[a]Route 1: (a) 10% $PdCl_2$(dppf)·DCM, 2 M Na_2CO_3, DME, MW, 120 °C; (b) $ArB(OR)_2$, 10% $PdCl_2$(dtbpf), 2 M Na_2CO_3, DME, MW, 120 °C. Route 2: (a) 10% $PdCl_2$(dppf)·DCM, 2 M Na_2CO_3, DME, MW, 120 °C; (b) 10% $PdCl_2$(dtbpf), 2 M Na_2CO_3, DME, MW, 120 °C.

Scheme 3. General Syntheses of Aminopyridine Analogues[a]

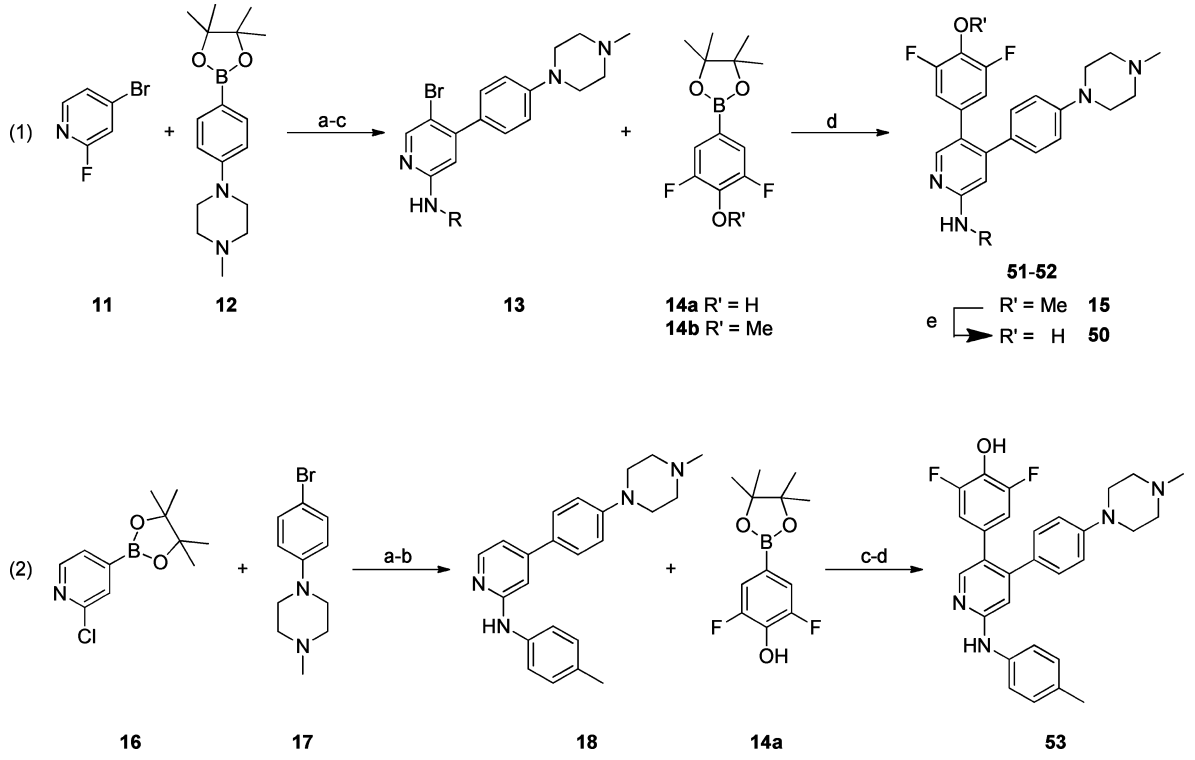

[a]Route 1: (a) 10% $PdCl_2$(dppf)·DCM, 2 M Na_2CO_3, DME, MW, 120 °C; (b) RNH_2.HCl, DIEA, 2-propanol, 150 °C; (c) Br_2, DCM, Na_2CO_3 rt; (d) 10% $PdCl_2$(dppf)·DCM, 2 M Na_2CO_3, DME, MW, 120 °C; (e) BBr_3, DCM, rt. Route 2: (a) 10% $PdCl_2$(dppf)·DCM, 2 M Na_2CO_3, DME, MW, 120 °C; (b) *p*-toluidine, $Pd_2(dba)_3$, BINAP, sodium-*tert*-butoxide, toluene, 110 °C, on; (c) NBS, $CHCl_3$, rt; (d) 10% $PdCl_2$(dppf)·DCM, 2 M Na_2CO_3, DME, MW, 120 °C.

hydrogen bonds in the hinge with the carbonyl oxygen of Asp148 and amide of Leu150. The compound is bound to an inactive conformation of the kinase that is partially similar to the type II, "DFG-out" conformations seen with compounds such as Gleevec bound to Abl.[18,19] Phe212 of the DFG-motif is flipped out as is observed in classical type II costructures; however, in contrast to Abl bound to Gleevec, the side chain of Asp211 occludes access to the hydrophobic pocket normally created by the displacement of the phenylalanine side chain. The Asp211 side chain forms a hydrogen bond to one of the phenols in **1** while making a salt bridge to the catalytic lysine, Lys100.

Structure–Activity Relationship and Selectivity Hypothesis. To provide potential optimization paths for the pyrazole hit **1** by scaffold morphing, the active enantiomer of the previously described RSK inhibitor BI-D1870 (**25**) was crystallized with RSK2 (Figure 4, left). A similar compound with the same bicyclic core but different substituents had previously been crystallized in PLK1 (Figure 4, right), where the 2-amino-

DOI: 10.1021/acs.jmedchem.5b00450
J. Med. Chem. XXXX, XXX, XXX−XXX

Scheme 4. General Syntheses of Aminopyrimidine Analogues[a]

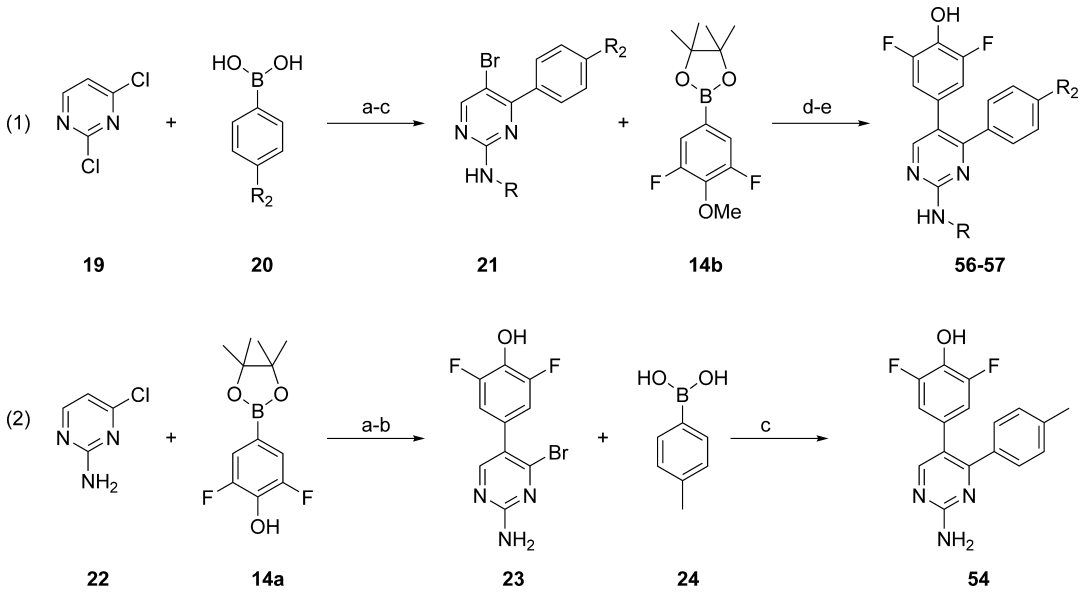

[a]Route 1: (a) 10% $PdCl_2$(dppf)·DCM, 2 M Na_2CO_3, DME, MW, 120 °C; (b) RNH_2·HCl, DIEA, 2-propanol, 100 °C; (c) NBS, $CHCl_3$, rt; (d) 10% $PdCl_2$(dppf)·DCM, 2 M Na_2CO_3, DME, MW, 120 °C; (e) BBr_3, DCM, rt. Route 2: (a) NBS, $CHCl_3$, rt; (b) 10% $PdCl_2$(dppf)·DCM, 2 M Na_2CO_3, DME, MW, 120 °C; (c) 10% $PdCl_2$(dppf)·DCM, 2 M Na_2CO_3, DME, MW, 120 °C.

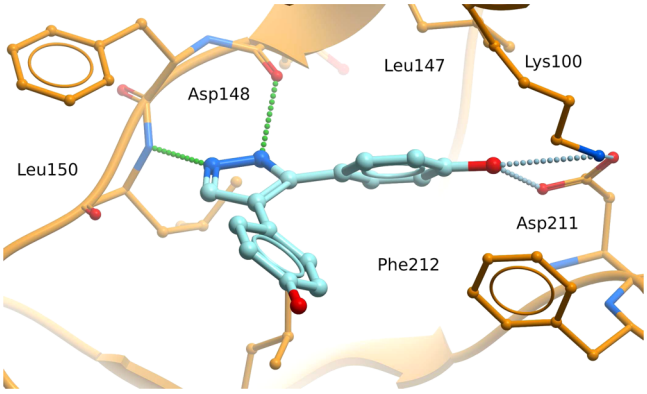

Figure 3. Co-crystal structure of **1** in RSK2.

pyrimidine moiety hydrogen bonds to the more exposed GateKeeper+3 (GK+3) carbonyl and GK+3 backbone NH of the hinge, which is typical for 2-aminopyrimidines in kinases. Surprisingly, in the RSK2 crystal structure the bicyclic core in **25** has flipped (Figure 4, left). While the pyrimidine nitrogen hydrogen bonds to the equivalent GK+3 backbone NH as in the PLK1 complex, the 2-amino group of **25** in RSK2 now hydrogen bonds to the more buried GK+1 carbonyl of the hinge. This orientation directs the difluorophenyl moiety toward Asp211, as observed in the crystal structure of **1** bound to RSK2 (Figure 5, superimposition of **25** and **1** bound to RSK2). We reasoned that the difluorophenol in **25** may be responsible for the unusual binding mode observed and might be a special pharmacophore preferred by RSK2 in the gatekeeper area. Superimposition of **1** and **25** (Figure 5) suggested a straightforward incorporation of two fluorines to the phenol of **1** which yielded a 4-fold potency enhancement (**29**).

Another unusual feature of the crystal structure of **25** in RSK2 (Figure 4, left) is the nonplanar conformation of the 2-arylamino moiety relative to the bicyclic core (dihedral angle of 52 degrees). However, quantum mechanical optimization suggests that the

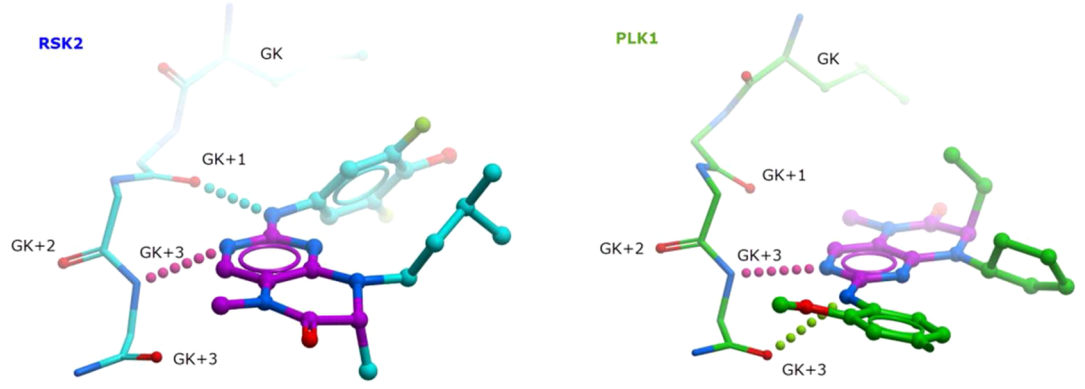

Figure 4. Compounds sharing the same bicyclic core (in magenta) crystallized in RSK2 (left, **25**, in cyan) and PLK1 (right, green, PDB code 2RKU). The hydrogen bond from pyrimidine nitrogen to Gatekeeper+3 (GK+3) backbone NH is common to both binding modes and is rendered as a magenta dotted line. Amino acid side chains have been hidden for clarity.

DOI: 10.1021/acs.jmedchem.5b00450
J. Med. Chem. XXXX, XXX, XXX−XXX

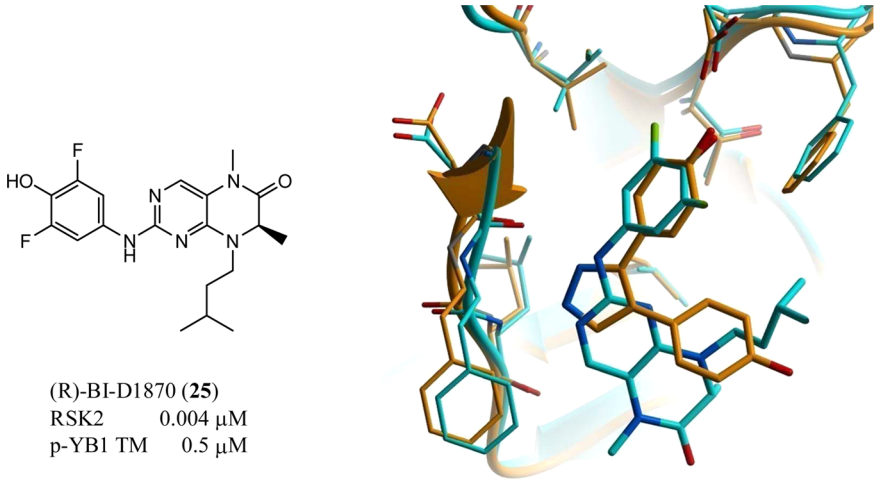

Figure 5. Crystal structures of **25** (cyan) and **1** (orange) bound to RSK2.

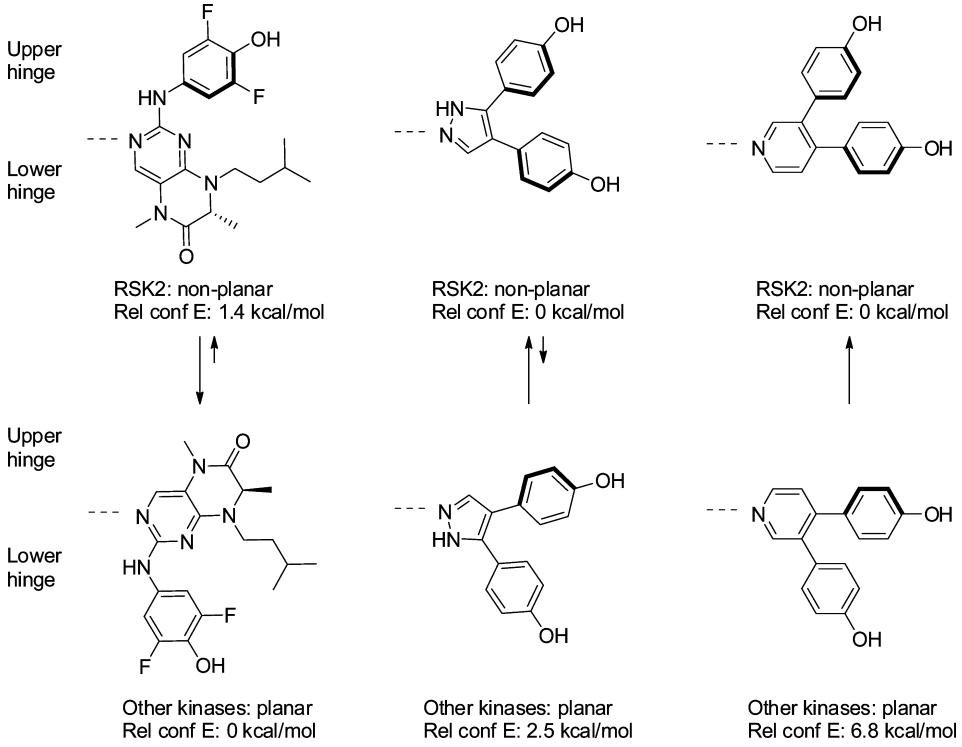

Figure 6. Conformational hypothesis of **25**, **1**, and **2** for selectivity optimization.

bound, nonplanar conformation is a higher energy conformation: 1.4 kcal/mol higher in energy than the unbound state where the arylamino and bicyclic core are coplanar (Figure 6). When the same scaffold was crystallized in PLK1 (Figure 4, right), the 2-arylamino substituent was coplanar with the bicyclic core. These observations suggested that while **25** binds in an unusual nonplanar mode in RSK2, it can adopt a conventional binding mode in other kinases in a planar conformation which would be consistent with the off-target kinase activities of **25** including potent PLK1 inhibition at 0.1 μM.[20]

We reasoned that the good kinase selectivity observed in **1** was due to placement of the phenol moiety at a similarly unusual angle in the gatekeeper area of RSK2 but attached to a scaffold which is less likely to adopt a coplanar conformation and thus may not be accommodated in other kinase pockets in a flipped binding mode. Quantum mechanical optimization[21] yields a propeller-shaped unbound state for **1**, with an energy penalty of 2.5 kcal/mol for adopting a conformation where the pyrazole ring and the C3-phenol are coplanar (Figure 6). Consequently, to further optimize kinase selectivity, our strategy aimed to penalize coplanarity while retaining similar 3D placement of the pharmacophores. We hypothesized that by expanding the pyrazole ring to pyridine, the penalty for coplanarity would be significantly increased due to the narrower angle between the substituent vectors. While potency might be lost due to a loss of a hinge hydrogen bond, a gain in selectivity was anticipated.

To gain an understanding of the essential pharmacophores, the SAR of the pyrazole series was investigated. The single phenol analogues, **26** and **27** (Table 1), were synthesized to determine if each of the phenols contributed equally to RSK2 potency. The phenol at R_1 (**26**) contributed significantly more to the potency (20×) than the phenol at R_2 (**27**, Table 1). An additional 3-fold

DOI: 10.1021/acs.jmedchem.5b00450
J. Med. Chem. XXXX, XXX, XXX−XXX

Table 1. Structure–Activity Relationship of the Pyrazole Series

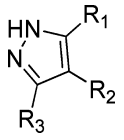

Compound	R_1	R_2	R_3	RSK2 IC_{50} (μM)	p-YB1 TM EC_{50} (μM)
1	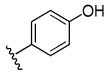	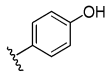	H	0.024	2.8
26	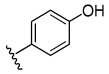		H	0.15	>20
27		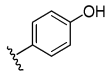	H	2.5	>20
28	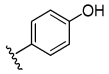		NH_2	0.053	3.2
29	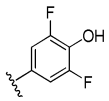	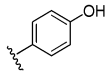	H	0.006	1.4

biochemically potency improvement could be realized with the addition of an amine at R_3 (**28**). Finally, as was suggested by the overlay of compound **1** and **25**, incorporating flanking difluoro substituents on the phenol (**29**) gave a 4-fold gain in potency over the starting hit **1**. Addition of the two fluorines both increases hydrophobic contacts in the partially hydrophobic pocket observed crystallographically and potentially influences the hydrogen bonding potential of the phenol hydroxy group, based on pK_a values cited in the literature.[22] The crystal structures of **1** and **25** bound to RSK2 showed that in the bioactive form the phenolic hydroxyl group is likely an un-ionized hydrogen bond donor to the Asp211 carboxyl group. The measured pK_a values of the phenols of **1** are 9 and 10.4, whereas literature pK_a values cited for difluorophenols are much lower: ~7. The experimental pK_a value for the 2,6-difluoro phenol in **29**, the fluorinated counterpart of **1**, is 6.5, which is in the same range as the literature data. This demonstrates that while the anticipated pK_a reduction also took place in our series, there is sufficient fraction of the compound in the un-ionized bioactive form.

To further increase the out of plane nature of the two phenyl rings, the 5-membered pyrazole core was expanded to 6-membered heterocyclic pyridine and pyrimidine cores (Tables 2–4). Modeling of these ring systems demonstrated the same binding mode as the pyrazole and that the key hydrogen bonds should overlap well. This was later confirmed with cocrystal structures. The pyridyl analogue **2** of the initial HTS hit **1**, however, exhibited a loss in potency which was hypothesized to be due to the loss of the hydrogen bond donor that the pyrazole contained. Despite the change in biochemical potency, the cellular target modulation effect of **1** and **2** against p-YB1 is virtually identical. Analysis of Caco-2 assay data suggested that both are highly permeable; however, **1** exhibited efflux which may explain the similar cellular target modulation of **1** and **2** despite compound **2** being 7-fold less potent. Incorporation of the flanking fluorines to the phenol (**30**) led to a 4-fold improvement in potency which mirrors the result seen in the pyrazole series, again presumably due to the increased acidic nature of the phenol in **30**. The hydroxyl on the C-4 phenyl group (**31**) could be removed with negligible effect on potency. The phenyl ring on the C-4 position of the pyridine ring was replaced with saturated heterocycles and alkyl groups. The tetrahydropyran (**32**) was tolerated, whereas the piperidine (**33**) and isopropyl (**34**) moieties led to significant losses in RSK2 potency.

A variety of moieties and substitution patterns were evaluated on the C4 phenyl group (R_2). In general, ortho substituted moieties led to less active analogues.[23] Meta substituents, however, were tolerated and, in some cases, dramatically improved the potency. Small substituents at the meta position such as methyl (**35**) and methoxy (**36**) resulted in potency similar to that of the unsubstituted phenyl (**31**), whereas larger groups such the aminoethoxy (**37**), 4-pyrazolo (**38**), morpholino (**39**), and methylpiperazino (**40**) provided a substantial boost in

DOI: 10.1021/acs.jmedchem.5b00450
J. Med. Chem. XXXX, XXX, XXX–XXX

Table 2. Structure−Activity Relationship of the Pyridine Series

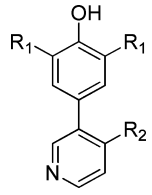

Compound	R_1	R_2	RSK2 IC_{50} (μM)	p-YB1 TM EC_{50} (μM)	Compound	R_1	R_2	RSK2 IC_{50} (μM)	p-YB1 TM EC_{50} (μM)
2	H		0.18	9.3	**40**	F		0.004	1.1
30	F		0.050	6.4	**41**	F		0.094	10.4
31	F		0.060	4.2	**42**	F		0.007	1.6
32	F		0.13	2.2	**43**	F		0.008	1.1
33	F		2.1	>20	**44**	F		0.020	2.1
34	F		0.78	>20	**45**	F		0.006	0.14
35	F		0.032	4.1	**46**	F		0.005	0.34
36	F		0.046	5.6	**47**	F		0.004	0.21
37	F		0.004	0.49	**48**	F		0.080	5.3
38	F		0.005	1.1	**49**	Cl		4.8	>20
39	F		0.018	2.3					

biochemical and cellular target modulation potency. The potency improvements in **37** and **38** may be due to the ability of the amines to reach the ribose binding site comprising Asp154, Glu197, and Asn198. The meta substituted morpholino (**39**) and methyl piperazino (**40**) compounds were also well-tolerated giving a 3-fold potency improvement versus **31**.

At the para position, the fluoro on the phenyl (**41**) was similarly potent as the unsubstituted phenyl (**31**), whereas methyl (**42**) and methoxy (**43**) moieties gave 7−8-fold improvements in potency, possibly due to the hydrophobic interaction with Phe79 in the P-loop. Amides were tolerated, exemplified here with the methyl amide **44**. In an effort to improve the solubility of this series, solubilizing groups at the para position were incorporated (**45**−**47**). The piperizine moieties provided, not surprisingly, the greatest solubility improvement with **45**, 6-times more soluble than **31** and **46**,

DOI: 10.1021/acs.jmedchem.5b00450
J. Med. Chem. XXXX, XXX, XXX−XXX

Table 3. Structure–Activity Relationship of the Aminopyridine Series

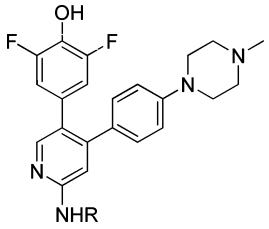

Compound	R	RSK2 IC_{50} (μM)	p-YB1 TM EC_{50} (μM)
50	H	0.006	0.44
51	Me	0.014	0.58
52	*iso*-Bu	0.022	2.5
53		0.006	0.69

Table 4. Structure–Activity Relationship of the Aminopyrimidine Series

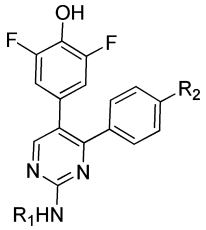

Compound	R_1	R_2	RSK2 IC_{50} (μM)	p-YB1 TM EC_{50} (μM)
54	H	Me	0.010	0.36
55	Me	Me	0.013	0.69
56	*i*-Pr	Me	0.023	1.5
57	*i*-Pr		0.020	0.61

and over 70-times more soluble than **31** with a solubility of 944 μM (in PBS buffer at pH 7.0). These examples showed at least a 10-fold improvement in biochemical potency with submicromolar p-YB1 target modulation activity in cells. The biochemical potency improvements may be due to increased hydrophobic contacts with the P-loop and its Phe79, as observed in the crystal structure of **46** bound to RSK2 where an ethyl moiety of the piperazine makes a hydrophobic contact with the Phe79 and Phe212 (Figure 7). Overall, substitution at the para position of the R_2 phenyl ring was found to give the best combination of biochemical and cellular target modulation potency.

Heterocycles at R_2 were also explored and found to be tolerated with methoxypyridine **48**, 10-fold less potent than the methoxyphenyl analogue **43**. Finally, in order to determine whether the fluorines on the phenol could be replaced with other halogens, the analogous dichlorophenol analogue of **41** (**49**) was synthesized, which led to a dramatic lost in potency (>50-fold). The loss in potency may be due to the larger steric bulk of the chlorines in a narrow area of the pocket where the chlorines could clash with inflexible amino acid residues from the hydrophobic core of the kinase (Val131). Further decreased hydrogen bonding potential of the phenol may also contribute to the loss of potency.

Analysis of the crystal structure of **46** bound to RSK2 (Figure 7) suggested that a hydrogen bond donor moiety substituted off of the core of the molecule could make an additional hydrogen bond with the backbone of Leu150 and provide a substituent vector toward the lower hinge for additional interactions to potentially further modulate potency, selectivity, and other properties. The aminopyridine analogue of **46** (**50**) was equipotent, consistent with the notion that hydrogen bonds do not always add potency but demonstrating that substitution was tolerated. Additional interactions with the hydrophobic region II/lower hinge[24] (residues Leu74, Gly153, and Leu200 in RSK2) were attempted with aliphatic and aromatic substituents in analogues **51**–**53**, including substituents such as **52** which are not coplanar with the hinge binding core. Such substituents have, in some cases, increased kinase selectivity due to varying degrees of protein flexibility in this region. For example, a similar strategy was utilized for ERK2 inhibitors which improved selectivity against three other kinases.[25] In the case of RSK2, no improvement in potency was realized with hydrophobic substituents relative to unsubstituted **50** which already demonstrated a good selectivity profile against an in-house kinase panel.

One of the concerns with the aminopyridine series was that they would not realize their full potency potential because a significant fraction of the pyridine nitrogen would be protonated at pH 7.4, and the protonated form would not be capable of binding to the RSK2 hinge. Earlier versions of MoKa[26] used for pK_a predictions in the design process suggested high pK_a values for 2-aminoalkylpyridines, for example, in **51** the pyridine nitrogen was predicted to have a pK_a of 7.0. In contrast, 2-aminopyrimidines were predicted to be essentially unprotonated at physiological pH, with pK_a values of 3–4. Consequently, the aminopyrimidine series (Table 4) was explored, and the aminopyrimidine analogue of **42** (**54**) displayed promising enzymatic and cell potencies with the cellular target modulation activity improved 4-fold. A small alkyl substituent off the amino (**55**) was equipotent to the unsubstituted amine **54**, while **56**, an isopropyl moiety, was 4-fold less potent in the p-YB1 target modulation cellular assay; however, incorporating a methyl piperazine off of the C4 phenyl (**57**) restored much of the p-YB1 activity. Overall, the SAR trends paralleled those of the aminopyridine series. Retrospective experimental measurements diminished the concern about the role of basicity in influencing binding to RSK2 at neutral pH. 2-Aminopyridine **50** had a pK_a value of 5.8 at the pyridine nitrogen which correlates to less than 10% of the protonated form being present under the assay conditions. As predicted, aminopyrimidines such as **56** with a measured value at 3.2 were significantly less basic, in line with the expected basicity reduction trend between aminopyridines and aminopyrimidines.

Discussion on the Selectivity of Analogues. The goal of this program was to deliver a potent and selective pan RSK tool compound to explore the importance of RSK in cancer. The initial bis-phenolpyrazole hit (**1**) had impressive starting selectivity against an in house panel of 69 kinases and in a further assessment of binding activity in a Kinome*Scan* panel of 96 kinases (Figure 8). In comparison, **25** bound to significantly

DOI: 10.1021/acs.jmedchem.5b00450
J. Med. Chem. XXXX, XXX, XXX–XXX

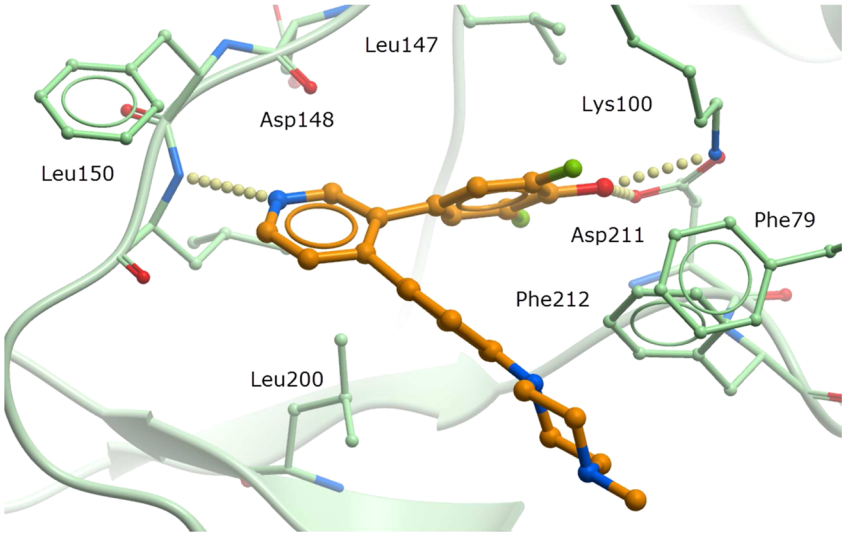

Figure 7. Co-crystal structure of **46** with RSK (PDB ID: 4NUS).

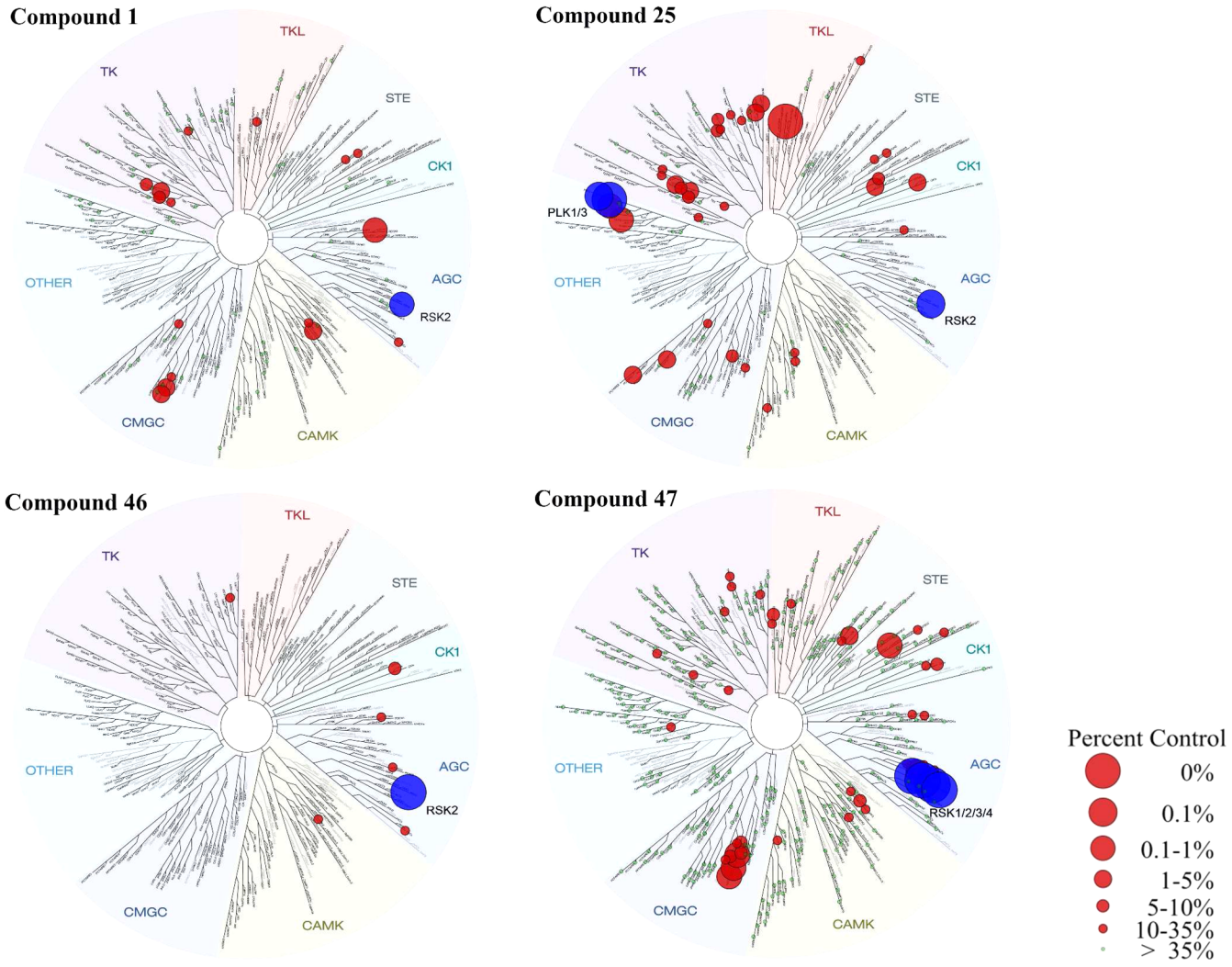

Figure 8. Kinome*Scan* panel of **1**, **25**, **46**, and **47** at 10 μM. All compounds tested against 96 kinases except for compound **47**, which was tested against 442 kinases. The image was generated using TREEspot Software Tool and is reprinted with permission from KINOMEscan, a division of DiscoveRx Corporation. Copyright DiscoveRx Corporation 2010. RSK refers to the N-terminal kinase domain for all RSK isoforms.

more kinases in the Kinome*Scan* panel including PLK. Compound **46** demonstrated improved potency compared to that of **1** and considerable improvement in selectivity by a Kinome*Scan* panel (96 kinases) compared to that of both **1** and

DOI: 10.1021/acs.jmedchem.5b00450
J. Med. Chem. XXXX, XXX, XXX−XXX

25. For confirmation, **47** was then profiled against the Kinome*Scan* panel of 442 kinases. Compound **47** showed no evidence of binding to PLK like **25** did and exhibited superior selectivity despite being tested on 4-times the number of kinases compared to that of **25** (Figure 8).[16] Further as can be seen in Figure 8 for **47**, compound **47** binds to all four RSK isoforms providing the pan-RSK activity desired in a tool compound.[16,27] This corroborated our in house enzymatic data which indicated that this series inhibited RSK1, 2, and 3 isoforms equally.[28]

In Vitro and in Vivo ADME. When we chose **1** as our lead compound to develop selective RSK biological probes, we understood that the phenol moiety would most likely limit their application to biochemical and cell based assays. We, however, did evaluate the ADME properties of **46** in vitro and in vivo. In rat liver microsomes, the in vitro clearance of **46** was high (170 μL/min/mg). In a single dose plasma pharmacokinetics in male Sprague−Dawley rats following i.v. administration, **46** displayed high clearance (166 mL/min/kg) and a short plasma half-life ($t_{1/2}$ 13 min). The volume of distribution (V_{ss}) was 1.6 L/kg suggesting moderate tissue drug distribution. Following oral dosing, oral exposure was poor. This data confirmed that while useful as in vitro biological probes, the series would not be useful as in vivo tools.

CONCLUSIONS/SUMMARY

Herein, we describe the optimization of a singleton HTS hit utilizing multiple approaches, including X-ray crystallography to optimize on-target potency, conformational analyses to develop a kinase selectivity hypothesis, and scaffold morphing. From these efforts, two potent and soluble difluorophenol pyridines (**46** and **47**) were developed with the desired selectivity profile. These compounds provide, for the first time, the ability to rigorously dissect RSK signaling and to evaluate RSK as an oncology target.

EXPERIMENTAL METHODS

Chemistry. All reagents and solvents were of commercial quality and used without further purification. Normal phase column chromatography was performed using Merck silica gel 60 (230−400 mesh) on automated ISCO instruments. The compounds and/or intermediates were characterized by high performance liquid chromatography (HPLC) using a Waters Millennium chromatography system with a 2695 Separation Module (Milford, MA). The analytical columns were reversed phase Phenomenex Luna C18, 5 μm, 4.6 × 50 mm, from Alltech (Deerfield, IL). A gradient elution was used (flow 2.5 mL/min), typically starting with 5% acetonitrile/95% water and progressing to 100% acetonitrile over a period of 10 min. All solvents contained 0.1% trifluoroacetic acid (TFA). All compounds where biological data are presented have >95% purity as determined by HPLC. Mass spectrometric analysis employed a Waters System (Alliance HT) HPLC, and a Micromass ZQ mass spectrometer for the LCMS instrument, an Eclipse XDB-C18, 2.1 × 50 mm for the chromatography column, and a solvent system that was a 5−95% gradient of acetonitrile in water with 0.05% TFA over a 4 min period (flow rate 0.8 mL/min; molecular weight range 200−1500; cone voltage 20 V; column temperature 40 °C). All masses were reported as those of the protonated parent ions. pK_a PRO capillary electrophoresis system (Advanced Analytical Technologies, Inc.) equipped with 96 uncoated fused-silica capillaries (75 μm i.d., 200 μm o.d.), UV detection at 214 nm at 20 °C was used for pK_a measurements. Compounds were obtained as 10 mM samples in DMSO and lyophilized to remove DMSO, and a commercial dilution buffer containing 0.2% DMSO was added. Premade buffer trays with 24 points (pH 1.75−11.2) were purchased from Advanced Analytical Technologies, Inc. The program pK_a Estimator (Advanced Analytical Technologies, Inc.) was used to calculate the pK_a values of compounds from the electrophoresis data. ^{1}H and ^{13}C NMR spectra of all compounds were recorded at 300 and 75 MHz, respectively. ^{1}H shifts are referenced to the residual protonated solvent signal (δ 7.25 for $CDCl_3$), and ^{13}C shifts are referenced to the deuterated solvent signal (δ 77 for d3-$CDCl_3$). Compound **1** was a purchased compound.

Synthesis of 4-(4-Phenyl-1*H*-pyrazol-3-yl)phenol (26). To 3-bromo-1*H*-pyrazole (100 mg, 0.68 mmol) in 3 mL of DMF was added NIS (152 mg, 0.68 mmol), and the reaction mixture was stirred at rt overnight. The reaction mixture was partitioned between ethyl acetate and water. The organic layer was dried over sodium sulfate, filtered, and concentrated. The crude product was purified by column chromatography (0−40% ethyl acetate in heptane) to give 3-bromo-4-iodo-1*H*-pyrazole (170 mg, 92%). ^{1}H NMR (300 MHz, $CDCl_3$) δ 7.57 (s, 1H), 10.80 (br s, 1H). LCMS (*m*/*z*) 272.8, 274.8 (MH^+), R*t* 0.66 min; UPLC 0.70 min.

To 3-bromo-4-iodo-1*H*-pyrazole (100 mg, 0.37 mmol) in DCM (3 mL) was added DIEA (0.19 mL, 1.10 mmol) and di*tert*-butyl dicarbonate (0.13 mL, 0.55 mmol). A catalytic amount of DMAP was added, and the reaction was stirred at rt for 1 h. The reaction was then partitioned between DCM and water. The organic layer was separated and washed with sat. NaCl. The organic layer was dried with sodium sulfate, filtered, and concentrated to give 137 mg of *tert*-butyl 3-bromo-4-iodo-1*H*-pyrazole-1-carboxylate (quantitative yield) which was used crude in the next step. LCMS (*m*/*z*) 372.8, 374.8, R*t* 1.04 min; UPLC 1.07 min.

To *tert*-butyl 3-bromo-4-iodo-1*H*-pyrazole-1-carboxylate (100 mg, 0.27 mmol) in DME (3 mL) and 2 M sodium carbonate (0.75 mL, 1.50 mmol) was added phenylboronic acid (49.0 mg, 0.40 mmol) and [1,1′-bis(diphenylphosphino)ferrocene]dichloropalladium(II)·DCM (219 mg, 0.27 mmol). The reaction mixture was heated in a microwave at 130 °C for 20 min. The crude reaction mixture was partitioned between ethyl acetate and water, and the organic layer was separated and washed with sat. NaCl. The organic layer was dried over sodium sulfate, filtered, and concentrated. The crude product was used in the next reaction. LCMS (*m*/*z*) 222.9, 224.9, R*t* 0.78 min and minor at 322.9, 324.9, R*t* 1.1 min. The crude product was dissolved in DCM (3 mL), then di*tert*-butyl dicarbonate (0.062 mL, 0.27 mmol) and DIEA (0.094 mL, 0.54 mmol) were added. A catalytic amount of DMAP was added, and the reaction mixture was stirred at rt for 1 h. The reaction mixture was partitioned between DCM and water. The organic layer was separated, washed with sat. NaCl, dried over sodium sulfate, filtered, and concentrated. The crude product was purified by column chromatography (0−30% ethyl acetate in heptane) to give *tert*-butyl 3-bromo-4-phenyl-1*H*-pyrazole-1-carboxylate (60 mg, purity 67%; 46% yield). LCMS (*m*/*z*) 323.0, 325.0, R*t* 1.13 min; UPLC 1.14 min.

To *tert*-butyl 3-bromo-4-phenyl-1*H*-pyrazole-1-carboxylate (30 mg, 0.062 mmol) in DME (2 mL) and 2 M sodium carbonate (0.5 mL, 1.00 mmol) was added (4-hydroxyphenyl)boronic acid (25.7 mg, 0.19 mmol) and [1,1′-bis(diphenylphosphino)ferrocene]dichloropalladium-(II)·DCM (5.1 mg, 6.22 μmol). The reaction mixture was heated in a microwave at 130 °C for 20 min, and then the reaction mixture was partitioned between ethyl acetate and water. The organic layer was separated, washed with sat. NaCl, and dried over sodium sulfate, filtered, and concentrated. LCMS shows a mixture of the product with and without the Boc protecting group: product without Boc, LCMS (*m*/*z*) 237.1, R*t* 0.69 min and with Boc, LCMS (*m*/*z*) 337.1, R*t* 1.04 min. To the crude product was added 30% TFA in DCM, and the reaction was stirred for 30 min at rt. The reaction mixture was concentrated and purified by reverse phase HPLC to give **26** (3.5 mg, 4.5% yield) as the TFA salt. LCMS (*m*/*z*) 237.1, R*t* 0.70 min; UPLC 2.62 min. HRMS found *m*/*z* 237.1029; $C_{15}H_{13}N_2O$ requires 237.1028.

Synthesis 4-(3-Phenyl-1*H*-pyrazol-4-yl)phenol (27). To 3-bromo-1*H*-pyrazole (100 mg, 0.68 mmol), phenylboronic acid (166 mg, 1.36 mmol) in DME (2 mL), and 2 M sodium carbonate (0.5 mL, 1.00 mmol) was added 1,1′-bis(diphenylphosphino)ferrocene]-dichloropalladium(II)·DCM (55.6 mg, 0.07 mmol), and the reaction mixture was heated in a microwave at 120 °C for 10 min. Two additional equivalents of phenylboronic acid (166 mg, 1.36 mmol) and 0.1 equiv of 1,1′-bis(diphenylphosphino)ferrocene]dichloropalladium(II)·DCM (55.6 mg, 0.07 mmol) were added. The reaction mixture was heated at 130 °C for 20 min. LCMS indicated that the desired product and starting

DOI: 10.1021/acs.jmedchem.5b00450
J. Med. Chem. XXXX, XXX, XXX−XXX

material were in a 1:1 ratio. Additional 1,1′-bis(diphenylphosphino)-ferrocene]dichloropalladium(II)·DCM (55.6 mg, 0.07 mmol) was added, and the reaction was heated 20 min more at 130 °C. The reaction was repeated on the same scale and was heated at 130 °C for 45 min. Starting material and desired product were present in 1:9 ratio. The reaction mixtures were combined, diluted with ethyl acetate, and washed with water and sat. NaCl. The organic layer was dried over sodium sulfate, filtered, and concentrated. The crude material was purified by column chromatography (0−50% ethyl acetate in heptane). The purification resulted in poor separation with phenyl boronic acid as the major peak. The desired product, 3-phenyl-1*H*-pyrazole, constituted approximately 26% of the material with starting material making up 9%. The impure 3-phenyl-1*H*-pyrazole (combined weigh 200 mg) was used in the next reaction. LCMS (*m*/*z*) 145.0, R*t* 0.65 min; UPLC 0.63 min.

To 3-phenyl-1*H*-pyrazole (200 mg, 0.42 mmol) in DMF (2 mL) was added NBS (81 mg, 0.46 mmol), and the reaction mixture was stirred at rt for 1 h. The reaction mixture was partitioned between ethyl acetate and water. The organic layer was separated, dried over sodium sulfate, filtered, and concentrated. The crude material was purified by column chromatography (0−40% ethyl acetate in heptane) to give 4-bromo-3-phenyl-1*H*-pyrazole (80.0 mg, 86% yield based on purity of starting material). LCMS (*m*/*z*) 222.9, 224.9, R*t* 0.79 min.

To 4-bromo-3-phenyl-1*H*-pyrazole (50 mg, 0.22 mmol) in DME (2 mL) and 2 M sodium carbonate (0.5 mL, 1.00 mmol) was added (4-hydroxyphenyl)boronic acid (61.8 mg, 0.45 mmol) and 1,1′-bis-(diphenylphosphino)ferrocene]dichloropalladium(II)·DCM (18.3 mg, 0.02 mmol). The reaction mixture was heated in a microwave at 130 °C for 20 min. The reaction was incomplete, so additional (4-hydroxyphenyl)boronic acid (30.9 mg, 0.22 mmol) and 1,1′-bis-(diphenylphosphino)-ferrocene]dichloropalladium(II)·DCM (18.3 mg, 0.02 mmol) were added, and the reaction mixture was heated to 130 °C in a microwave for 30 min. The reaction mixture was partitioned between ethyl acetate and water, and the organic layer was separated, dried over sodium sulfate, filtered, and concentrated. The crude product was purified by reverse phase HPLC to give **27** (5.3 mg, 10.0% yield). LCMS (*m*/*z*) 237.1, R*t* 0.64 min; UPLC 2.51 min. HRMS found *m*/*z* 237.1031; $C_{15}H_{13}N_2O$ requires 237.1028.

Synthesis of 4-(5-Amino-4-phenyl-1*H*-pyrazol-3-yl)phenol (28). Methyl 4-hydroxybenzoate (1.00 g, 6.57 mmol) and potassium carbonate (1.36 g, 9.86 mmol) were dissolved in acetone (26 mL), and then benzyl bromide (0.860 mL, 7.23 mmol) was added and stirred at 60 °C overnight. The reaction mixture was concentrated, and then water was added to give a white solid. The solid was filtered and dried on high-vac overnight to give methyl 4-(benzyloxy)benzoate (1.59 g, quantitative yield). LCMS (*m*/*z*) 243.0, R*t* 1.05 min.

Benzyl cyanide (200 mg, 1.71 mmol) was dissolved in THF (7 mL), and sodium hydride (119 mg, 2.97 mmol) was added. Methyl 4-(benzyloxy)benzoate (300 mg, 1.24 mmol) in THF (10 mL) was added, and the reaction was stirred at 60 °C overnight. The reaction was quenched with sat. aq. NH_4Cl and extracted with ethyl acetate. The organic layer was dried with $MgSO_4$, filtered, and concentrated. The crude material was purified by column chromatography (0−100% ethyl acetate in heptane) to give 3-(4-(benzyloxy)phenyl)-3-oxo-2-phenyl-propanenitrile (270.7 mg, 67% yield). LCMS (*m*/*z*) 328.1, R*t* 1.07 min.

3-(4-(Benzyloxy)phenyl)-3-oxo-2-phenylpropanenitrile (135 mg, 0.41 mmol) was dissolved in ethanol (5 mL) and acetic acid (5 mL), and then hydrazine (0.207 mL, 6.60 mmol) was added. The reaction mixture was stirred at 90 °C for 3 h and then diluted in ethyl acetate and sat. aq. sodium bicarbonate. The phases were separated, and the organic layer was washed with sat. NaCl, dried with $MgSO_4$, filtered, and concentrated. The crude material was purified by column chromatography [0−100% (10% methanol in ethyl acetate) with heptane] to give 5-(4-(benzyloxy)phenyl)-4-phenyl-1*H*-pyrazol-3-amine (141 mg, 100% yield). LCMS (*m*/*z*) 342.2, R*t* 0.86 min.

5-(4-(Benzyloxy)phenyl)-4-phenyl-1*H*-pyrazol-3-amine (141 mg, 0.41 mmol) was dissolved in ethanol (20 mL), and the solution was purged for 15 min with nitrogen. Then, 10% Pd/C (88 mg, 0.08 mmol) was added to the solution and placed under an atmosphere of H_2. The reaction was stirred at rt overnight. The reaction mixture was filtered through Celite, then concentrated. The crude material was purified by reverse phase HPLC and lyophilized to give **28** as the TFA salt, (29.9 mg, 28% yield). ^{1}H NMR (400 MHz, DMSO-d_6) δ 6.66 (d, *J* = 8.61 Hz, 2H), 7.05 (d, *J* = 8.61 Hz, 2H), 7.16 (d, *J* = 6.65 Hz, 2H), 7.19−7.27 (m, 1H), 7.31 (t, *J* = 7.24 Hz, 2H). LCMS (*m*/*z*) 252.1, R*t* 0.54 min; UPLC 1.80 min. HRMS found *m*/*z* 252.1138; $C_{15}H_{14}N_3O$ requires 252.1137.

Synthesis of 2,6-Difluoro-4-(4-(4-hydroxyphenyl)-1*H*-pyrazol-3-yl)phenol (29). To 4-bromo-2,6-difluorophenol (**3**, 100 mg, 0.48 mmol) in DME (3 mL) and 2 M sodium carbonate (0.75 mL, 1.50 mmol) was added (1*H*-pyrazol-3-yl)boronic acid (**4**, 161 mg, 1.44 mmol) and 1,1′-bis(diphenylphosphino)ferrocene]dichloropalladium-(II)·DCM (39.1 mg, 0.05 mmol). The reaction mixture was heated at 120 °C for 20 min in the microwave. A second reaction on the same scale was carried out, and both reactions were combined. The reaction mixture was diluted with ethyl acetate, separated, and concentrated. The crude material was then purified by column chromatography (0−80% ethyl acetate in heptane) to give 2,6-difluoro-4-(1*H*-pyrazol-3-yl)phenol (160 mg, 85% yield). LCMS (*m*/*z*) 197.0, R*t* 0.52 min.

To 2,6-difluoro-4-(1*H*-pyrazol-3-yl)phenol (160 mg, 0.82 mmol) in DMF (3 mL) was added NBS (131 mg, 0.73 mmol), and the reaction was stirred at rt for 1 h. The reaction mixture was diluted with ethyl acetate and washed with water. The organic layer was separated and concentrated and purified by column chromatography (0−70% ethyl acetate in heptane) to give 4-(4-bromo-1*H*-pyrazol-3-yl)-2,6-difluor-ophenol as a white solid (90 mg, 40% yield). LCMS (*m*/*z*) 274.9, 276.9, R*t* 0.68 min.

To 4-(4-bromo-1*H*-pyrazol-3-yl)-2,6-difluorophenol (40 mg, 0.14 mmol) in DME (2 mL) and 2 M sodium carbonate (0.5 mL, 1.00 mmol) was added (4-hydroxyphenyl)boronic acid (30.1 mg, 0.22 mmol) and 1,1′-bis(di*tert*-butylphosphino)ferrocene]dichloropalladium(II) (9.48 mg, 0.02 mmol). The reaction mixture was heated in a microwave at 120 °C for 15 min. The reaction mixture was concentrated, and the residue was dissolved in DMSO and purified twice by reverse phase HPLC to give **29** as the TFA salt (2.5 mg, 6% yield). ^{1}H NMR (400 MHz, DMSO-d_6) δ 6.55−6.78 (m, 2H), 6.82−7.10 (m, 5H), 7.51−7.73 (m, 1H), 9.22−9.45 (m, 1H), 10.05−10.40 (m, 1H). LCMS (*m*/*z*) 274.9, 288.9, R*t* 0.57 min, UPLC 1.77 min. HRMS found *m*/*z* 289.0787; $C_{15}H_{11}N_2O_2F_2$ requires 289.0789.

Synthesis of 4,4′-(Pyridine-3,4-diyl)diphenol (2). To a mixture of 4-bromo-3-chloropyridine (**8**, 100 mg, 0.52 mmol), 4-(4,4,5,5-tetramethyl-1,3,2-dioxaborolan-2-yl)phenol (343 mg, 1.56 mmol), and 2 M sodium carbonate (0.75 mL, 1.50 mmol) in DME (3 mL) was added 1,1′-bis(diphenylphosphino)ferrocene]dichloropalladium(II)·DCM (42.4 mg, 0.05 mmol). The reaction mixture was heated in a microwave at 120 °C for 15 min. Two additional equivs of 4-(4,4,5,5-tetramethyl-1,3,2-dioxaborolan-2-yl)phenol (229 mg, 1.04 mmol) and 0.1 equiv of 1,1′-bis(diphenylphosphino)ferrocene]dichloropalladium-(II)·DCM (42.4 mg, 0.05 mmol) were added, and the reaction mixture was heated at 130 °C for 25 min. The reaction mixture was diluted with ethyl acetate and washed with sat. NaCl. The organic layer was filtered and concentrated, and the residue was purified by reverse phase HPLC to give 4-(3-chloropyridin-4-yl)phenol as a TFA salt (60 mg, 56% yield). LCMS (*m*/*z*) 206.1, R*t* 0.47 min.

To 4-(3-chloropyridin-4-yl)phenol (70 mg, 0.34 mmol) in DME (2 mL) and 2 M sodium carbonate (0.5 mL, 1.00 mmol) were added (4-hydroxyphenyl)boronic acid (141 mg, 1.02 mmol) and 1,1′-bis-(diphenylphosphino)ferrocene]dichloropalladium(II)·DCM (27.8 mg, 0.03 mmol). The reaction mixture was heated in a microwave at 130 °C for 40 min. The crude reaction mixture was partitioned between ethyl acetate and water. The organic layer was separated, dried over sodium sulfate, filtered, and concentrated. The residue was purified by reverse phase HPLC to give **2** as the TFA salt (10.5 mg, 12% yield). ^{1}H NMR (300 MHz, DMSO-d_6) δ 6.57−6.82 (m, 4H), 6.85−7.17 (m, 4H), 7.50−7.73 (m, 1H), 8.47−8.77 (m, 3H), 9.42−9.98 (m, 2H). LCMS (*m*/*z*) 264.1, R*t* 0.43 min, UPLC 1.10 min. HRMS found *m*/*z* 264.1028; $C_{17}H_{14}NO_2$ requires 264.1025.

Synthesis of 2,6-Difluoro-4-(4-(4-hydroxyphenyl)pyridin-3-yl)phenol (30). To 4-chloro-3-(4,4,5,5-tetramethyl-1,3,2-dioxaborolan-2-yl)pyridine (**6**, 100 mg, 0.42 mmol) in DME (3 mL) were added 1,1′-bis(diphenylphosphino)ferrocene]dichloropalladium(II)·DCM (22.7 mg, 0.03 mmol), 2 M sodium carbonate (0.75 mL, 1.50 mmol),

DOI: 10.1021/acs.jmedchem.5b00450
J. Med. Chem. XXXX, XXX, XXX−XXX

and 4-bromo-2,6-difluorophenol (**5**, 58.2 mg, 0.28 mmol). The reaction mixture was heated at 120 °C for 12 min in a microwave. An identical reaction at the same scale was repeated, and the two reactions were combined. The reaction mixture was partitioned between ethyl acetate and water. The organic layer was separated, dried over sodium sulfate, filtered, and concentrated. The crude product (4-(4-chloropyridin-3-yl)-2,6-difluorophenol, 100 mg, 74% yield) was used in the next reaction. LCMS (*m*/*z*) 242.0, R*t* 0.53 min.

To 4-(4-chloropyridin-3-yl)-2,6-difluorophenol (30 mg, 0.12 mmol) in DME (2 mL) and 2 M sodium carbonate (0.75 mL, 1.50 mmol) were added (4-hydroxyphenyl)boronic acid (34.3 mg, 0.25 mmol) and 1,1′-bis(diphenylphosphino)ferrocene]dichloropalladium(II)·DCM (10.1 mg, 0.01 mmol), and the reaction mixture was heated in a microwave at 130 °C for 20 min. Additional (4-hydroxyphenyl)boronic acid (17.2 mg, 0.12 mmol) and 1,1′-bis(diphenylphosphino)ferrocene]-dichloropalladium(II)·DCM (10.1 mg, 0.01 mmol) were added. The reaction mixture was heated at 130 °C for 30 min in a microwave. The reaction mixture was partitioned between ethyl acetate and water, and the organic layer was separated, dried over sodium sulfate, filtered, and concentrated. The residue was purified by reverse phase HPLC to give **30** (5.1 mg, 3% yield) as the TFA salt. ^{1}H NMR (400 MHz, CD_3OD) δ 7.47 (m, 2H), 7.59−7.72 (m, 2H), 7.75−7.92 (m, 2H), 8.22−8.39 (m, 1H), 9.26−9.52 (m, 2H), 10.39−10.71 (m, 1H), 11.00−11.33 (m, 1H). LCMS (*m*/*z*) 300.0, R*t* 0.46 min, UPLC 1.20 min. HRMS found *m*/*z* 300.0837; $C_{17}H_{12}NO_2F_2$ requires 300.0836.

Synthesis of 2,6-Difluoro-4-(4-phenylpyridin-3-yl)phenol (31). To 4-bromo-2,6-difluorophenol (1.20 g, 5.74 mmol) and 4-chloro-3-(4,4,5,5-tetramethyl-1,3,2-dioxaborolan-2-yl)pyridine (1.38 g, 5.74 mmol) in DME (16 mL) and 2 M sodium carbonate (4.0 mL, 8.00 mmol) was added $PdCl_2$(dppf)·DCM (0.47 g, 0.57 mmol). The reaction mixture was heated in an oil bath at 100 °C for 3 h. The reaction mixture was diluted with EtOAc, filtered, and evaporated. The residue was triturated with DCM, and the solid was filtered and washed with DCM to provide 4-(4-chloropyridin-3-yl)-2,6-difluorophenol (996 mg, 72% yield). LCMS (*m*/*z*) 241.9, 242.9, 0.53 min.

Compound **31** was synthesized by the same method as **30** to give 20 mg (TFA salt, 17% yield). ^{1}H NMR (400 MHz, DMSO-d_6) δ 6.80 (m, 2H), 7.06−7.28 (m, 2H), 7.28−7.47 (m, 6H), 7.48−7.69 (m, 2H), 8.54−8.80 (m, 3H), 10.14−10.62 (m, 1H). LCMS (*m*/*z*) 284.0, R*t* 0.57 min, UPLC 2.17 min. HRMS found *m*/*z* 284.0890; $C_{17}H_{12}NOF_2$ requires 284.0887.

Synthesis of 2,6-Difluoro-4-(4-(tetrahydro-2*H*-pyran-4-yl)-pyridin-3-yl)phenol (32). A mixture of 4-(4-chloropyridin-3-yl)-2,6-difluorophenol (48 mg, 0.20 mmol), 2-(3,6-dihydro-2*H*-pyran-4-yl)-4,4,5,5-tetramethyl-1,3,2-dioxaborolane (50.1 mg, 0.24 mmol), Pd-(dtbpf)Cl_2 (12.9 mg, 0.02 mmol), and 2 M Na_2CO_3 (0.30 mL, 0.60 mmol) in 1,4-dioxane (4 mL) was heated in a microwave at 120 °C for 10 min. The reaction mixture was diluted with ethyl acetate (100 mL) and washed with sat. NaCl (20 mL). The organic layer was dried over $MgSO_4$, filtered, and concentrated. The residue was purified by column chromatography (5% methanol in 1:1 ethyl acetate and heptane) to give 4-(4-(3,6-dihydro-2*H*-pyran-4-yl)pyridin-3-yl)-2,6-difluorophenol (32 mg, 55% yield). LCMS (*m*/*z*) 290.0, R*t* 0.42 min.

4-(4-(3,6-Dihydro-2*H*-pyran-4-yl)pyridin-3-yl)-2,6-difluorophenol (22 mg, 0.08 mmol) was dissolved in MeOH (2 mL), and Pd/C (8.1 mg) was added. The flask was fitted with a 3-way stopcock, and the flask was evacuated under vacuum and then filled with H_2. The reaction was stirred under H_2 overnight, and then the reaction was flushed with N_2. The solid was removed by filtration, and the filtrate was concentrated under reduced pressure. The crude product was purified by reverse-phase HPLC to give **32** as the TFA salt (1.5 mg, 5% yield). ^{1}H NMR (400 MHz, CD_3OD) δ 1.67 (d, *J* = 12.91 Hz, 2H), 1.78−1.94 (m, 3H), 3.07−3.19 (m, 2H), 3.37 (dd, *J* = 11.74, 10.37 Hz, 2H), 3.98(dd, *J* = 11.54, 3.72 Hz, 2H), 6.97−7.09 (m, 2H), 7.94 (d, *J* = 6.06 Hz, 1H), 8.57 (s, 1H), 8.67 (d, *J* = 5.87 Hz, 1H). LCMS (*m*/*z*) 292.0, R*t* 0.42 min; UPLC 1.01 min. HRMS found *m*/*z* 292.1151; $C_{16}H_{16}NO_2F_2$ requires 292.1149.

Synthesis of 2,6-Difluoro-4-(4-(piperidin-4-yl)pyridin-3-yl)-phenol (33). A mixture of 4-(4-chloropyridin-3-yl)-2,6-difluorophenol (120 mg, 0.49 mmol), *tert*-butyl 4-(4,4,5,5-tetramethyl-1,3,2-dioxaborolan-2-yl)-5,6-dihydropyridine-1(2*H*)-carboxylate (184 mg, 0.60 mmol), Pd(dtbpf)Cl_2 (32.4 mg, 0.05 mmol), and Na_2CO_3 (2 M, 0.75 mL, 1.5 mmol) in 1,4-dioxane (5 mL) was stirred in microwave at 120 °C for 10 min. The reaction mixture was diluted with ethyl acetate (100 mL) and washed with sat. NaCl (20 mL). The organic layer was dried over $MgSO_4$, filtered, and concentrated. The residue was purified by column chromatography (5% methanol in 1:1 ethyl acetate and heptane) to give *tert*-butyl 4-(3-(3,5-difluoro-4-hydroxyphenyl)pyridin-4-yl)-5,6-dihydropyridine-1(2*H*)-carboxylate (145 mg, 75% yield). LCMS (*m*/*z*) 389.3, R*t* 0.66 min.

tert-Butyl 4-(3-(3,5-difluoro-4-hydroxyphenyl)pyridin-4-yl)-5,6-dihydropyridine-1(2*H*)-carboxylate (125 mg, 0.32 mmol) was dissolved in MeOH (5 mL), and Pd/C (68.5 mg, 0.06 mmol) was added. The flask was fitted with a 3-way stopcock, and the flask was evacuated under vacuum and then filled with H_2. The reaction was stirred under H_2 for 4 h, and then the reaction was flushed with N_2. The solid was removed by filtration, and the filtrate was concentrated to give the crude *tert*-butyl 4-(3-(3,5-difluoro-4-hydroxyphenyl)pyridin-4-yl)piperidine-1-carboxylate (105 mg, yield 84%) which was used directly in the next reaction. LCMS (*m*/*z*) 391.1, R*t* 0.68 min.

A mixture of *tert*-butyl 4-(3-(3,5-difluoro-4-hydroxyphenyl)pyridin-4-yl)piperidine-1-carboxylate (70 mg, 0.18 mmol) in DCM (4 mL) and TFA (1 mL) was stirred at rt for 2 h. The solvents were removed, and the crude product was purified by reverse phase HPLC to **33** as the TFA salt (45 mg, 62% yield). ^{1}H NMR (400 MHz, CD_3OD) δ 2.00 (d, *J* = 6.85 Hz, 5H), 2.69−2.94 (m, 4H), 3.00 (br. s., 3H), 3.18 (br. s., 2H), 3.44 (d, *J* = 12.52 Hz, 3H), 6.88−7.12 (m, 2H), 7.76 (br. s., 2H), 8.54 (s, 1H), 8.67 (br. s., 2H); LCMS (*m*/*z*) 291.1, R*t* 0.25 min, UPLC 0.32 min. HRMS found *m*/*z* 291.1307; $C_{16}H_{17}N_2OF_2$ requires 291.1309.

Synthesis of 2,6-Difluoro-4-(4-isopropylpyridin-3-yl)phenol (34). To a mixture of 4-(4-chloropyridin-3-yl)-2,6-difluorophenol (50 mg, 0.21 mmol) and 4,4,5,5-tetramethyl-2-(prop-1-en-2-yl)-1,3,2-dioxaborolane (174 mg, 1.04 mmol) in 2 M sodium carbonate (1.04 mL, 2.07 mmol) and dioxane (2.1 mL) was added Pd(dtbpf)Cl_2 (22.9 mg, 0.03 mmol). The reaction mixture was heated in a microwave at 120 °C for 15 min. The reaction mixture was diluted with ethyl acetate, dried over $MgSO_4$, filtered, and concentrated. The crude 2,6-difluoro-4-(4-(prop-1-en-2-yl)pyridin-3-yl)phenol (51.2 mg) was used in the next reaction. LCMS (*m*/*z*) 248.0, R*t* 0.51 min.

The crude 2,6-difluoro-4-(4-(prop-1-en-2-yl)pyridin-3-yl)phenol (51.2 mg, 0.21 mmol) was dissolved in MeOH (4.1 mL) and then purged with N_2 for 5 min. Pd/C (22.0 mg, 0.02 mmol) was added, and the reaction was placed under an atmosphere of H_2 and stirred overnight at rt. The reaction was then flushed with N_2. The reaction mixture was filtered through a pad of Celite and then concentrated. The residue was purified by reverse phase HPLC to give **34** as a TFA salt (8.8 mg, 17% yield). ^{1}H NMR (400 MHz, CD_3OD) δ 1.17 (d, *J* = 7.04 Hz, 6H), 3.16 (t, *J* = 6.85 Hz, 1H), 6.90−6.96 (m, 2H), 7.88 (d, *J* = 5.87 Hz, 1H), 8.48 (s, 1H), 8.58 (d, *J* = 6.26 Hz, 1H). LCMS (*m*/*z*) 250.1, R*t* 0.52 min; UPLC 1.63 min. HRMS found *m*/*z* 250.1041; $C_{14}H_{14}NOF_2$ requires 250.1043.

Synthesis of 2,6-Difluoro-4-(4-(m-tolyl)pyridin-3-yl)phenol (35). To 4-(4-chloropyridin-3-yl)-2,6-difluorophenol (40 mg, 0.166 mmol) (for synthesis see **30**, step 1) in DME (2 mL) and 2 M sodium carbonate (0.5 mL, 1.0 mmol) were added *m*-tolylboronic acid (33.8 mg, 0.248 mmol) and Pd(dtbpf)Cl_2 (10.8 mg, 0.017 mmol). The reaction mixture was heated in a microwave at 120 °C for 12 min. The reaction mixture was partitioned between ethyl acetate and water, and the organic layer was separated, dried over sodium sulfate, filtered, and concentrated. The residue was purified by reverse phase HPLC to give **35** (14 mg, 28% yield) as a TFA salt. ^{1}H NMR (400 MHz, DMSO-d_6) δ 2.22 (s, 3H), 6.61−6.96 (m, 3H), 6.98−7.26 (m, 3H), 7.38−7.62 (m, 1H), 8.40−8.79 (m, 2H), 10.11−10.54 (m, 1H). LCMS (*m*/*z*) 298.0, R*t* 0.65 min, UPLC 2.32 min. HRMS found *m*/*z* 298.1046; $C_{18}H_{14}NOF_2$ requires 298.1043.

Synthesis of 2,6-Difluoro-4-(4-(3-methoxyphenyl)pyridin-3-yl)phenol (36). Compound **36** was synthesized by the same method as **35** as a TFA salt (13.2 mg, TFA salt, 25% yield). ^{1}H NMR (400 MHz, DMSO-d_6) δ 3.67 (s, 3H), 6.58−7.04 (m, 5H), 7.11−7.37 (m, 1H), 7.46−7.65 (m, 1H), 8.51−8.77 (m, 2H), 10.13−10.55 (m, 1H). LCMS

DOI: 10.1021/acs.jmedchem.5b00450
J. Med. Chem. XXXX, XXX, XXX−XXX

(m/z) 314.0, Rt 0.61 min, UPLC 2.04 min. HRMS found m/z 314.0988; $C_{18}H_{14}NO_2F_2$ requires 314.0993.

Synthesis of 4-(4-(3-(2-Aminoethoxy)phenyl)pyridin-3-yl)-2,6-difluorophenol (37). A mixture of 4-chloro-3-(4,4,5,5-tetramethyl-1,3,2-dioxaborolan-2-yl)pyridine (1.40 g, 5.85 mmol), 5-bromo-1,3-difluoro-2-methoxybenzene (1.43 g, 6.43 mmol), $PdCl_2$(dppf)·DCM (477 mg, 0.58 mmol), and 2 M sodium carbonate (8.8 mL, 17.5 mmol) in 1,4-dioxane (8 mL) was heated in a microwave at 120 °C for 10 min. The reaction mixture was diluted with ethyl acetate (150 mL) and washed with sat. NaCl (20 mL). The organic was dried over $MgSO_4$, filtered, and concentrated. The residue was purified by column chromatography (5% methanol in 1:1 ethyl acetate and heptane) to provide 4-chloro-3-(3,5-difluoro-4-methoxyphenyl)pyridine (1.23 m, 82% yield). LCMS (m/z) 255.9, 257.9, Rt 0.78 min.

To a mixture of 4-chloro-3-(3,5-difluoro-4-methoxyphenyl)pyridine (60 mg, 0.24 mmol), 3-hydroxyphenylboronic acid (64.7 mg, 0.47 mmol) in 2 M sodium carbonate (0.82 mL, 1.6 mmol) and dioxane (1.6 mL) was added Pd(dtbpf)Cl_2 (25.9 mg, 0.04 mmol). The reaction was heated in a microwave at 120 °C for 15 min. The reaction mixture was diluted with ethyl acetate, dried over $MgSO_4$, filtered, and concentrated. The crude was purified by column chromatography (0−100% ethyl acetate/heptane to give 3-(3-(3,5-difluoro-4-methoxyphenyl)pyridin-4-yl)phenol (15.1 mg, 21% yield). LCMS (m/z) 314.1, Rt 0.63 min.

3-(3-(3,5-Difluoro-4-methoxyphenyl)pyridin-4-yl)phenol (15.1 mg, 0.05 mmol) was dissolved in DMF (0.48 mL). Sodium hydride (5.8 mg, 0.14 mmol) was added. After 5 min, *tert*-butyl 2-bromoethylcarbamate (32.4 mg, 0.14 mmol) was added, and the reaction was stirred at rt for 6 h. The reaction was heated at 50 °C overnight. The reaction mixture was diluted with ethyl acetate and washed with sat. NaCl. The organic layer was dried over $MgSO_4$, filtered, and concentrated. The crude *tert*-butyl 2-(3-(3-(3,5-difluoro-4-methoxyphenyl)pyridin-4-yl)phenoxy)-ethylcarbamate (22 mg) was used in the next reaction. LCMS (m/z) 457.1, Rt 0.86 min

To a solution of *tert*-butyl 2-(3-(3-(3,5-difluoro-4-methoxyphenyl)-pyridin-4-yl)phenoxy)ethylcarbamate (22 mg, 0.05 mmol) in DCM (2 mL) was added BBr_3 (1 M, 0.15 mL, 0.15 mmol). The reaction was stirred in a sealed vial at rt for 45 min. The reaction mixture was quenched with Et_3N (12 equiv) and then diluted with ethyl acetate, dried over $MgSO_4$, filtered, and concentrated. The crude product was purified by reverse phase HPLC to give **37** as a TFA salt (6.2 mg, 38% yield). ^{1}H NMR (400 MHz, CD_3OD) δ 3.24 (br. s., 2H), 4.07 (t, J = 4.89 Hz, 2H), 6.66−6.74 (m, 2H), 6.79−6.86 (m, 2H), 6.94−7.01 (m, 1H), 7.23−7.31 (m, 1H), 7.61 (d, J = 5.48 Hz, 1H), 8.54−8.63 (m, 2H). LCMS (m/z) 343.0, Rt 0.41 min, UPLC 1.15 min. HRMS found m/z 343.1257; $C_{19}H_{17}N_2O_2F_2$ requires 343.1258.

Synthesis of 4-(4-(3-(1*H*-Pyrazol-4-yl)phenyl)pyridin-3-yl)-2,6-difluorophenol (38). A mixture of 4-chloro-3-(3,5-difluoro-4-methoxyphenyl)pyridine (150 mg, 0.59 mmol) (see **37** for synthesis) and 3-hydroxyphenylboronic acid (162 mg, 1.17 mmol) was dissolved in 2 M sodium carbonate (2.9 mL, 5.9 mmol) and DME (5.8 mL) and purged with nitrogen. Pd(dtbpf)Cl_2 (57.4 mg, 0.09 mmol) was added, and the vial was sealed and heated in a microwave at 120 °C for 15 min. The reaction mixture was diluted with ethyl acetate and washed with sat. NaCl. The organic was dried over $MgSO_4$, filtered, and concentrated. The crude mixture was purified by column chromatography (0−100% ethyl acetate/heptane) to provide 3-(3-(3,5-difluoro-4-methoxyphenyl)pyridin-4-yl)phenol (135 mg, 73% yield). LCMS (m/z) 314.0, Rt 0.62 min.

3-(3-(3,5-Difluoro-4-methoxyphenyl)pyridin-4-yl)phenol (60 mg, 0.19 mmol) was dissolved in Et_3N (80 μL, 0.58 mmol) and DCM (1.9 mL). 1,1,1-Trifluoro-*N*-phenyl-*N*-(trifluoromethylsulfonyl)-methanesulfonamide (75 mg, 0.21 mmol) was added, and the reaction was stirred at rt for 2 h. The reaction mixture was diluted with DCM and washed with sat. NaCl. The organic layer was dried over $MgSO_4$, filtered, and concentrated to give 3-(3-(3,5-difluoro-4-methoxyphenyl)pyridin-4-yl)phenyl trifluoromethanesulfonate (85 mg), which was used crude in the next step. LCMS (m/z) 446.0, Rt 0.70 min.

A mixture of 3-(3-(3,5-difluoro-4-methoxyphenyl)pyridin-4-yl)-phenyl trifluoromethanesulfonate (60 mg, 0.14 mmol), *tert*-butyl 4-(4,4,5,5-tetramethyl-1,3,2-dioxaborolan-2-yl)-1*H*-pyrazole-1-carboxylate (59.4 mg, 0.20 mmol), and 2 M sodium carbonate (112 mg, 1.35 mmol) in DME (3.0 mL) was purged with N_2, and $PdCl_2$(dppf)·DCM (16.5 mg, 0.02 mmol) was added. The reaction was heated in a microwave at 120 °C for 15 min. The reaction mixture was diluted with ethyl acetate and washed with sat. NaCl. The organic layer was dried over $MgSO_4$, filtered, and concentrated. The crude product was purified by column chromatography (0−100% ethyl acetate/heptane) to give 4-(3-(1*H*-pyrazol-4-yl)phenyl)-3-(3,5-difluoro-4-methoxyphenyl)-pyridine (35.6 mg, 73% yield). LCMS (m/z) 364.0, Rt 0.63 min.

4-(3-(1*H*-Pyrazol-4-yl)phenyl)-3-(3,5-difluoro-4-methoxyphenyl)-pyridine (47.6 mg, 0.13 mmol) was dissolved in DCM (2 mL), and boron tribromide (1 M, 0.66 mL, 0.66 mmol) was added. The reaction was stirred at rt overnight. The reaction mixture was diluted with DCM and washed with sat. NaCl. A solid was filtered and found to be the desired product. The organic layer which also contained the desired product was dried over $MgSO_4$, filtered, and concentrated. The crude product from both the organic layer and the precipitate were purified separately by reverse phase HPLC to give **38** as a TFA salt (29.3 mg, 64% yield). ^{1}H NMR (400 MHz, DMSO-d_6) δ 6.82−6.92 (m, 3H), 7.26 (t, J = 7.73 Hz, 1H), 7.47 (t, J = 1.66 Hz, 1H), 7.51−7.57 (m, 1H), 7.62 (d, J = 5.28 Hz,1H), 7.93 (s, 2H), 8.63−8.69 (m, 2H). LCMS (m/z) 350.0, Rt 0.50 min; UPLC 1.60 min. HRMS found m/z 350.1106; $C_{20}H_{14}N_3OF_2$ requires 350.1105.

Synthesis of 2,6-Difluoro-4-(4-(3-morpholinophenyl)pyridin-3-yl)phenol (39). Compound **39** was synthesized by the same method as **35** to give 13.4 mg (TFA salt, 21% yield). ^{1}H NMR (400 MHz, DMSO-d_6) δ 2.87−3.10 (m, 4H), 3.64−3.94 (m, 4H), 6.48−6.69 (m, 1H), 6.69−7.01 (m, 4H), 7.09−7.30 (m, 1H), 7.46−7.67 (m, 1H), 8.49−8.79 (m, 2H), 10.15−10.51 (m, 1H). LCMS (m/z) 369.1, Rt 0.55 min; UPLC 1.82 min. HRMS found m/z 369.1411; $C_{21}H_{19}N_2O_2F_2$ requires 369.1415.

Synthesis of 2,6-Difluoro-4-(4-(3-(4-methylpiperazin-1-yl)-phenyl)pyridin-3-yl)phenol (40). To 4-(4-Chloropyridin-3-yl)-2,6-difluorophenol (50 mg, 0.21 mmol) in DME (2 mL) and 2 M sodium carbonate (0.50 mL, 1.00 mmol) were added *tert*-butyl 4-(3-(4,4,5,5-tetramethyl-1,3,2-dioxaborolan-2-yl)phenyl)piperazine-1-carboxylate (161 mg, 0.41 mmol) and bis(di-*tert*-butylphosphino)ferrocene dichloropalladium(II) (13.5 mg, 0.02 mmol). The reaction mixture was heated in a microwave at 120 °C for 15 min. The crude reaction mixture was partitioned between ethyl acetate and water. The organic layer was separated and evaporated to give the crude product. LCMS (m/z) 468.1, Rt 0.78 min. To the crude product was added 2 mL of 30% TFA in DCM, and it was stirred at rt for 1 h. The reaction was concentrated, and the crude product was purified by reverse phase HPLC to provide 2,6-difluoro-4-(4-(3-(piperazin-1-yl)phenyl)pyridin-3-yl)phenol as a TFA salt (20 mg, 26% yield). LCMS (m/z) 368.0, Rt 0.40 min.

To 2,6-difluoro-4-(4-(3-(piperazin-1-yl)phenyl)pyridin-3-yl)phenol (13 mg, 0.04 mmol) in MeOH (3 mL) was added formaldehyde (10.6 mg, 0.35 mmol) and acetic acid (0.02 mL, 0.35 mmol). After 5 min, sodium triacetoxyborohydride (22.5 mg, 0.11 mmol) was added. The reaction mixture was stirred at rt for 2 h. The reaction was concentrated and purified by reverse phase HPLC to provide **40** (4 mg, 29% yield) as the TFA salt. ^{1}H NMR (400 MHz, DMSO-d_6) δ 2.70−2.97 (m, 5H), 2.98−3.21 (m, 2H), 3.34−3.60 (m, 2H), 3.67−3.87 (m, 2H), 6.47−6.72 (m, 2H), 6.73−6.91 (m, 2H), 6.92−7.05 (m, 1H), 7.10−7.31 (m, 1H), 7.36−7.57 (m, 1H), 8.46−8.73 (m,1H), 9.46−9.79 (m, 1H), 10.18−10.48 (m, 1H). LCMS (m/z) 382.0, Rt 0.41 min; UPLC 1.16 min. HRMS found m/z 382.1736; $C_{22}H_{22}N_3OF_2$ requires 382.1731.

Synthesis of 2,6-Difluoro-4-(4-(4-fluorophenyl)pyridin-3-yl)-phenol (41). Compound **41** was synthesized by the same method as **30** to provide 11.6 mg (TFA salt, 20% yield). ^{1}H NMR (400 MHz, DMSO-d_6) δ 6.81 (m, 2H), 7.10−7.35 (m, 4H), 7.38−7.63 (m, 1H), 8.47−8.78 (m, 2H), 10.12−10.56 (m, 1H). LCMS (m/z) 302.0, Rt 0.60 min; UPLC 2.03 min. HRMS found m/z 302.0794; $C_{17}H_{11}NOF_3$ requires 302.0793.

Synthesis of 2,6-Difluoro-4-(4-(*p*-tolyl)pyridin-3-yl)phenol (42). Compound **42** was synthesized by the same method as **35** to provide 9.1 mg (TFA salt, 18% yield). ^{1}H NMR (400 MHz, DMSO-d_6) δ 2.28 (s, 3H), 2.47 (s, 6H), 6.72−6.97 (m, 2H), 6.97−7.32 (m, 4H),

DOI: 10.1021/acs.jmedchem.5b00450
J. Med. Chem. XXXX, XXX, XXX−XXX

7.43−7.66 (m, 1H), 8.65 (s, 2H), 10.13−10.59 (m, 1H). LCMS (*m*/*z*) 298.0, R*t* 0.65 min; UPLC 2.37 min. HRMS found *m*/*z* 298.1047; $C_{18}H_{14}NOF_2$ requires 298.1043.

Synthesis of 2,6-Difluoro-4-(4-(4-methoxyphenyl)pyridin-3-yl)phenol (43). Compound **43** was synthesized by the same method as **35** to provide 16.2 mg (TFA salt, 31% yield). ^{1}H NMR (400 MHz, DMSO-d_6) δ 3.66−3.86 (m, 4H), 6.69−7.03 (m, 4H), 7.05−7.27 (m, 2H), 7.40−7.68 (m, 1H), 8.45−8.78 (m, 2H), 10.22−10.53 (m, 1H). LCMS (*m*/*z*) 314.0, R*t* 0.60 min, UPLC 2.01 min. HRMS found *m*/*z* 314.0990; $C_{18}H_{14}NO_2F_2$ requires 314.0993.

Synthesis of 4-(3-(3,5-Difluoro-4-hydroxyphenyl)pyridin-4-yl)-*N*-methylbenzamide (44). Compound **44** was synthesized by the same method as **30** to provide 5.3 mg (TFA salt, 20% yield). ^{1}H NMR (400 MHz, DMSO-d_6) δ 2.64−2.78 (m, 3H), 6.67−6.88 (m, 2H), 7.13−7.33 (m, 2H), 7.34−7.56 (m, 1H), 7.62−7.82 (m, 2H), 8.33−8.53 (m, 1H), 8.50−8.71 (m, 2H), 10.17−10.45 (m, 1H). LCMS (*m*/*z*) 341.0, R*t* 0.40 min, UPLC 1.03 min.

Synthesis of 2,6-Difluoro-4-(4-(4-(piperazin-1-yl)phenyl)-pyridin-3-yl)phenol (45). To 4-(4-chloropyridin-3-yl)-2,6-difluorophenol (50 mg, 0.21 mmol) in DME (2 mL) and 2 M sodium carbonate (0.50 mL, 1.00 mmol) were added *tert*-butyl 4-(4-(4,4,5,5-tetramethyl-1,3,2-dioxaborolan-2-yl)phenyl)piperazine-1-carboxylate (96 mg, 0.25 mmol) and Pd(dtbpf)Cl_2 (13.5 mg, 0.02 mmol). The reaction mixture was heated in a microwave at 120 °C for 12 min. The reaction mixture was partitioned between ethyl acetate and water. The organic layer was separated and concentrated to give the crude product. LCMS (*m*/*z*) 468.2, R*t* 0.78 min. To the crude product was added 30% TFA in DCM (2 mL). The reaction was stirred 30 min at rt, and then the reaction was concentrated. The crude was purified by reverse phase HPLC to provide **45** (19.5 mg, 26% yield). ^{1}H NMR (400 MHz, DMSO-d_6) δ 8.61−8.74 (m, 1H), 8.55−8.59 (m, 1H), 8.51−8.55 (m, 1H), 7.38−7.46 (m, 1H), 7.04−7.11 (m, 2H), 6.90−6.97 (m, 2H), 6.80−6.86 (m, 2H), 3.30−3.39 (m, 4H), 3.13−3.25 (m, 4H). LCMS (*m*/*z*) 368.1, R*t* 0.37 min; UPLC 0.83 min. HRMS found *m*/*z* 368.1575; $C_{21}H_{20}N_3OF_2$ requires 368.1574.

Synthesis of 2,6-Difluoro-4-(4-(4-(4-methylpiperazin-1-yl)-phenyl)pyridin-3-yl)phenol (46). Compound **46** was synthesized by the same method as **45** to provide 40.1 mg (TFA salt, 10% yield). ^{1}H NMR (400 MHz, DMSO-d_6) δ 10.19−10.45 (m, 1H), 9.44−9.73 (m, 1H), 8.36−8.63 (m, 2H), 7.31−7.51 (m, 1H), 6.99−7.14 (m, 2H), 6.67−6.99 (m, 4H), 3.74−3.98 (m, 3H), 2.84−3.18 (m, 5H), 2.70−2.84 (m, 3H). LCMS (*m*/*z*) 382.1, R*t* 0.38 min; UPLC 0.85 min. HRMS found *m*/*z* 382.1733; $C_{22}H_{22}N_3OF_2$ requires 382.1731.

Synthesis of 2,6-Difluoro-4-(4-(4-morpholinophenyl)pyridin-3-yl)phenol (47). Compound **47** was synthesized by the same method as **35** to provide 65.2 mg (TFA salt, 21% yield). ^{1}H NMR (400 MHz, DMSO-d_6) δ 3.07−3.28 (m, 5H), 6.77−7.01 (m, 4H), 7.03−7.24 (m, 2H), 7.53−7.81 (m, 1H), 8.50−8.78 (m, 2H), 10.24−10.66 (m, 1H). LCMS (*m*/*z*) 369.0, R*t* 0.57 min; UPLC 1.91 min. HRMS found *m*/*z* 369.1415; $C_{21}H_{19}N_2O_2F_2$ requires 369.1415.

Synthesis of 2,6-Difluoro-4-(6-methoxy-[3,4′-bipyridin]-3′-yl)phenol (48). Compound **48** was synthesized by the same method as **35** to provide 13.1 mg (TFA salt, 26% yield). ^{1}H NMR (400 MHz, DMSO-d_6) δ 3.85 (s, 3H), 6.68−6.86 (m, 1H), 6.86−7.06 (m, 2H), 7.34−7.58 (m, 1H), 7.59−7.80 (m, 1H), 7.95−8.21 (m, 1H), 8.54−8.84 (m, 2H), 10.19−10.73 (m, 1H). LCMS (*m*/*z*) 315.0, R*t* 0.52 min; UPLC 1.53 min. HRMS found *m*/*z* 315.0942; $C_{17}H_{13}N_2O_2F_2$ requires 315.0945.

Synthesis of 2,6-Dichloro-4-(4-(4-fluorophenyl)pyridin-3-yl)-phenol (49). To 4-bromo-2,6-dichlorophenol (50 mg, 0.21 mmol), 4-chloro-3-(4,4,5,5-tetramethyl-1,3,2-dioxaborolan-2-yl)pyridine (54.5 mg, 0.23 mmol), and 2 M sodium carbonate (0.50 mL, 1.00 mmol) in DME (2 mL) was added $PdCl_2$(dppf)·DCM (16.9 mg, 0.02 mmol), and the reaction mixture was heated in a microwave at 120 °C for 12 min. The reaction mixture was partitioned between ethyl acetate and water. The organic layer was separated, dried over sodium sulfate, filtered, and concentrated to provide 2,6-dichloro-4-(4-chloropyridin-3-yl)phenol (56 mg) in quantitative yield. The crude product was used in the next step. LCMS (*m*/*z*) 273.9, 275.9, R*t* 0.68 min.

To 2,6-dichloro-4-(4-chloropyridin-3-yl)phenol (50 mg, 0.18 mmol) in DME (2 mL) and 2 M sodium carbonate (0.50 mL, 1.00 mmol) were added 4-fluorophenylboronic acid (38.2 mg, 0.27 mmol) and bis(di-*tert*-butylphosphino)ferrocene dichloropalladium(II) (11.9 mg, 0.02 mmol). The reaction mixture was heated in a microwave at 120 °C for 12 min. The crude reaction mixture was partitioned between ethyl acetate and water. The organic layer was separated, dried over sodium sulfate, filtered, and concentrated. The product was purified by reverse phase HPLC to provide **49** as a TFA salt (8.7 mg, 14% yield). ^{1}H NMR (400 MHz, DMSO-d_6) δ 7.18 (m, 6H), 7.44−7.59 (m, 1H), 8.51−8.75 (m, 3H), 10.22−10.45 (m, 1H). LCMS (*m*/*z*) 333.9, 335.8, R*t* 0.68 min; UPLC 2.54 min. HRMS found *m*/*z* 334.0199; $C_{17}H_{11}NOFCl_2$ requires 344.0202.

Synthesis of 4-(6-Amino-4-(4-(4-methylpiperazin-1-yl)-phenyl)pyridin-3-yl)-2,6-difluorophenol (50). To 5-bromo-1,3-difluoro-2-methoxybenzene (2.0 g, 8.97 mmol) in DME (20 mL) were added 4,4,4′,4′,5,5,5′,5′-octamethyl-2,2′-bi(1,3,2-dioxaborolane) (3.42 g, 13.45 mmol) and potassium acetate (2.64 g, 26.9 mmol). The mixture was purged with N_2 for 5 min, and then $PdCl_2$(dppf)·DCM (0.73 g, 0.90 mmol) was added. The reaction mixture was heated at 100 °C overnight. The product does not produce a mass ion in LCMS. UPLC shows two major peaks at 0.62 min (possibly boronic acid) and 1.19 min (possibly boronic ester) in a 1:1 ratio. The reaction mixture was diluted with ethyl acetate and washed with water. The organic layer was dried over sodium sulfate, filtered, and concentrated. The crude mixture was used in the next reaction.

To 5-bromo-4-chloropyridin-2-amine (70 mg, 0.34 mmol) and 2-(3,5-difluoro-4-methoxyphenyl)-4,4,5,5-tetramethyl-1,3,2-dioxaborolane (91 mg, 0.34 mmol) in DME (2 mL) and 2 M sodium carbonate (0.50 mL, 1.00 mmol) was added $PdCl_2$(dppf)·DCM (27.6 mg, 0.03 mmol). The reaction mixture was heated in a microwave at 120 °C for 15 min. The reaction mixture was partitioned between ethyl acetate and water. The organic layer was separated, dried over sodium sulfate, filtered, and concentrated. LCMS (*m*/*z*) 270.9, 272.8, R*t* 0.63 min. The crude 4-chloro-5-(3,5-difluoro-4-methoxyphenyl)pyridin-2-amine was used for the next step.

To 4-chloro-5-(3,5-difluoro-4-methoxyphenyl)pyridin-2-amine (70 mg, 0.26 mmol) and 1-methyl-4-(4-(4,4,5,5-tetramethyl-1,3,2-dioxaborolan-2-yl)phenyl)piperazine (94 mg, 0.31 mmol) in DME (2 mL) and 2 M sodium carbonate (0.50 mL, 1.00 mmol) was added Pd(dtbpf)Cl_2 (16.9 mg, 0.03 mmol). The reaction mixture was heated in a microwave at 120 °C for 15 min. The crude was partitioned between ethyl acetate and water. The organic layer was separated, dried over sodium sulfate, filtered, and concentrated. The crude material was purified by reverse phase HPLC to provide 5-(3,5-difluoro-4-methoxyphenyl)-4-(4-(4-methylpiperazin-1-yl)phenyl)pyridin-2-amine (60 mg, 56% yield) as the TFA salt. LCMS (*m*/*z*) 411.1, R*t* 0.51 min.

To 5-(3,5-difluoro-4-methoxyphenyl)-4-(4-(4-methylpiperazin-1-yl)phenyl)pyridin-2-amine in DCM (2 mL) was added BBr_3 (1 M, 0.78 mL, 0.78 mmol). The reaction was stirred at rt for 2 h. The reaction mixture was diluted with DCM, and sat. $NaHCO_3$ was added. A solid was observed and was filtered, which LCMS indicates is the product. The organic layer was separated and concentrated. The product from both the solid and the organic layer was purified by reverse phase HPLC to provide **50** as a TFA salt (21.3 mg, 21% yield over two steps). ^{1}H NMR (400 MHz, DMSO-d_6) δ 2.83 (s, 3H), 2.91−3.21 (m, 6H), 3.73−4.09 (m, 3H), 6.55−6.86 (m, 3H), 6.87−7.16 (m, 4H), 7.50−7.83 (m, 2H), 7.84−8.01 (m, 1H), 9.52−9.98 (m, 1H), 10.18−10.49 (m, 1H). LCMS (*m*/*z*) 397.1, R*t* 0.40 min; UPLC 1.14 min. HRMS found *m*/*z* 397.1843; $C_{22}H_{23}N_4OF_2$ requires 397.1840.

Synthesis of 2,6-Difluoro-4-(6-(methylamino)-4-(4-(4-methylpiperazin-1-yl)phenyl)pyridin-3-yl)phenol (51). To 4-bromo-2-fluoropyridine (**11**, 500 mg, 2.84 mmol) and 1-methyl-4-(4-(4,4,5,5-tetramethyl-1,3,2-dioxaborolan-2-yl)phenyl)piperazine (**12**, 1.03 g, 3.41 mmol) in DME (12 mL) and 2 M sodium carbonate (3 mL, 6.00 mmol) was added $PdCl_2$(dppf)·DCM (232 mg, 0.28 mmol). The reaction mixture was heated in a microwave at 120 °C for 15 min. The crude mixture was partitioned between ethyl acetate and water. The organic layer was separated, dried over sodium sulfate, filtered, and concentrated. The crude product was purified by column chromatog-

DOI: 10.1021/acs.jmedchem.5b00450
J. Med. Chem. XXXX, XXX, XXX−XXX

raphy (0−20% MeOH/DCM) to provide 1-(4-(2-fluoropyridin-4-yl)phenyl)-4-methylpiperazine as a light brown solid (850 mg, 80% yield, purity 75%). LCMS (*m*/*z*) 272.2, R*t* 0.52 min.

To 1-(4-(2-fluoropyridin-4-yl)phenyl)-4-methylpiperazine (100 mg, 0.37 mmol) in DMSO (2 mL) was added methanamine hydrochloride (124 mg, 1.84 mmol) and DIEA (0.32 mL, 1.84 mmol). The reaction mixture was heated at 130 °C overnight. Five equivalents each of methanamine hydrochloride and DIEA were added, and the reaction was heated at 150 °C for 48 h. The reaction mixture was partitioned between ethyl acetate and water. The organic layer was separated, and the aqueous layer was washed twice with ethyl acetate. The organic extracts were combined, washed with sat. NaCl, dried over sodium sulfate, filtered, and concentrated to provide crude *N*-methyl-4-(4-(4-methylpiperazin-1-yl)phenyl)pyridin-2-amine (100 mg, 99% yield, purity 60%) which was used in the next step without purification. LCMS (*m*/*z*) 283.2, R*t* 0.34 min.

To a mixture of *N*-methyl-4-(4-(4-methylpiperazin-1-yl)phenyl)-pyridin-2-amine (100 mg, 0.21 mmol) and sodium carbonate (27.0 mg, 0.26 mmol) in DCM (1 mL) and water (4 mL) was added bromine (10.9 μL, 0.21 mmol) in DCM (1 mL) at 0 °C. The reaction mixture was stirred for 1 h at 0 °C. The product was extracted twice with heptane. A solid was observed, which was filtered and washed with heptane. LCMS indicates that the solid is the starting material. The organic layer was separated, dried over sodium sulfate, filtered, and concentrated. The crude 5-bromo-*N*-methyl-4-(4-(4-methylpiperazin-1-yl)phenyl)-pyridin-2-amine (**13**) was used later in the synthesis. LCMS (*m*/*z*) 361.0, 363.0, R*t* 0.37 min.

To 4-bromo-2,6-difluorophenol (1.0 g, 4.78 mmol) in DME (20 mL) were added 4,4,4′,4′,5,5,5′,5′-octamethyl-2,2′-bi(1,3,2-dioxaborolane) (1.82 mg, 7.18 mmol) and potassium acetate (14.1 g, 14.4 mmol). The reaction mixture was purged with N_2 for 5 min, and then $PdCl_2$(dppf)·DCM (391 mg, 0.48 mmol) was added. The reaction was heated at 100 °C overnight. The product **14a** does not produce a mass ion in LCMS. By UPLC, the major peak had a retention time of 0.954 min. The crude reaction mixture was used in the next reaction.

To crude 2,6-difluoro-4-(4,4,5,5-tetramethyl-1,3,2-dioxaborolan-2-yl)phenol (**14a**, 32 mg, 0.12 mmol) in DME (1.2 mL) and 2 M sodium carbonate (0.3 mL, 0.60 mmol) were added 5-bromo-*N*-methyl-4-(4-(4-methylpiperazin-1-yl)phenyl)pyridin-2-amine (**13**, 30 mg, 0.08 mmol) and $PdCl_2$(dppf)·DCM (6.8 mg, 0.008 mmol). The reaction mixture was heated in a microwave at 120 °C for 15 min. The reaction mixture was concentrated, dissolved in DMSO, and purified twice by reverse phase HPLC to provide **51** as a TFA salt (10.2 mg, 30% yield). ^{1}H NMR (400 MHz, DMSO-d_6) δ 10.02−10.40 (m, 1H), 9.41−9.77 (m, 1H), 7.69−8.06 (m, 1H), 6.99−7.07 (m, 2H), 6.90−6.97 (m, 2H), 6.65−6.76 (m, 2H), 3.66−4.10 (m, 4H), 3.01−3.17 (m, 3H), 2.86−3.00 (m, 4H), 2.77−2.86 (m, 3H). LCMS (*m*/*z*) 411.1, R*t* 0.41 min; UPLC 1.22 min. HRMS found *m*/*z* 411.2000; $C_{23}H_{25}N_4OF_2$ requires 411.1996.

Synthesis of 2,6-Difluoro-4-(6-(isobutylamino)-4-(4-(4-methylpiperazin-1-yl)phenyl)pyridin-3-yl)phenol (52). Compound **52** was synthesized by the same method as **51** to provide 4.1 mg (TFA salt, 28% yield). ^{1}H NMR (400 MHz, DMSO-d_6) δ 0.83−0.99 (m, 6H), 1.74−1.93 (m, 1H), 2.76−2.86 (m, 3H), 2.86−3.00 (m, 3H), 3.00−3.19 (m, 4H), 3.70−4.06 (m, 4H), 6.65−6.75 (m, 3H), 6.90−6.97 (m, 2H), 6.98−7.06 (m, 2H), 7.69−7.97 (m, 1H), 9.45−9.81 (m, 1H), 10.03−10.40 (m, 1H). LCMS (*m*/*z*) 453.2, R*t* 0.56 min; UPLC 2.02 min. HRMS found *m*/*z* 453.2461; $C_{26}H_{31}N_4OF_2$ requires 453.2466.

Synthesis of 2,6-Difluoro-4-(4-(4-(4-methylpiperazin-1-yl)-phenyl)-6-(*p*-tolylamino)pyridin-3-yl) phenol (53). To 1-(4-bromophenyl)-4-methylpiperazine (**17**, 500 mg, 1.96 mmol) and 2-chloro-4-(4,4,5,5-tetramethyl-1,3,2-dioxaborolan-2-yl)pyridine (**16**, 516 mg, 2.16 mmol) in DME (12 mL) and 2 M sodium carbonate (3.0 mL, 6.0 mmol) was added $PdCl_2$(dppf)·DCM (160 mg, 0.20 mmol). The reaction was heated in a microwave at 120 °C for 15 min. The reaction mixture was partitioned between ethyl acetate and water. The organic layer was dried over sodium sulfate, filtered, and concentrated. The crude product was purified by column chromatography (0−20% MeOH/DCM) to obtain 1-(4-(2-chloropyridin-4-yl)phenyl)-4-methylpiperazine as a light brown solid (400 mg, 64% yield). LCMS (*m*/*z*) 288.0, R*t* 0.55 min.

To 1-(4-(2-chloropyridin-4-yl)phenyl)-4-methylpiperazine (70 mg, 0.24 mmol) in toluene (2 mL) was added *p*-toluidine (31.3 mg, 0.29 mmol), Pd_2(dba)$_3$ (22.3 mg, 0.02 mmol), BINAP (30.3 mg, 0.05 mmol), and sodium *tert*-butoxide (33.9 mg, 0.35 mmol). The reaction mixture was heated at 110 °C overnight. The reaction was concentrated, and the crude material was purified by reverse phase HPLC to provide 4-(4-(4-methylpiperazin-1-yl)phenyl)-*N*-*p*-tolylpyridin-2-amine as a TFA salt. The product was dissolved in methanol and treated with HCO_3 resin (2−3eq) at rt for 30 min, filtered, and evaporated to provide product as a free base (38 mg, 44% yield). LCMS (*m*/*z*) 359.2, R*t* 0.51 min.

To 4-(4-(4-methylpiperazin-1-yl)phenyl)-*N*-*p*-tolylpyridin-2-amine (**18**, 38 mg, 0.11 mmol) in $CHCl_3$ (2 mL) was added NBS (18.9 mg, 0.11 mmol). After stirring for 10 min at rt, the reaction mixture was partitioned between DCM and water. The organic layer was dried over sodium sulfate, filtered, and concentrated. The crude material was purified by reverse phase HPLC to provide 5-bromo-4-(4-(4-methylpiperazin-1-yl)phenyl)-*N*-*p*-tolylpyridin-2-amine (30 mg, 63% yield). LCMS (*m*/*z*) 437.1, 439.1, R*t* 0.73 min.

To 5-bromo-4-(4-(4-methylpiperazin-1-yl)phenyl)-*N*-*p*-tolylpyridin-2-amine (20 mg, 0.05 mmol) in DME (1 mL) and 2 M sodium carbonate (0.25 mL, 0.50 mmol) were added 2,6-difluoro-4-(4,4,5,5-tetramethyl-1,3,2-dioxaborolan-2-yl)phenol (17.6 mg, 0.07 mmol) and $PdCl_2$(dppf)·DCM (3.7 mg, 4.6 μmol). The reaction mixture was heated in a microwave at 120 °C for 10 min. The reaction mixture was diluted with DCM. The organic layer was dried over sodium sulfate, filtered, and concentrated. The crude material was purified by reverse phase HPLC to provide **53** as a TFA salt (5.5 mg, 21% yield). ^{1}H NMR (400 MHz, DMSO-d_6) δ 9.97−10.22 (m, 1H), 9.39−9.77 (m, 1H), 8.93−9.21 (m, 1H), 7.87−8.20 (m, 1H), 7.34−7.67 (m, 2H), 6.99−7.11 (m, 2H), 6.90−6.98 (m, 2H), 6.52−6.83 (m, 2H), 3.73−4.03 (m, 4H), 3.02−3.22 (m, 3H), 2.87−3.01 (m, 2H), 2.72−2.88 (m, 3H), 2.07−2.28 (m, 3H). LCMS (*m*/*z*) 487.2, R*t* 0.58 min; UPLC 2.33 min. HRMS found *m*/*z* 487.2312; $C_{29}H_{29}N_4OF_2$ requires 487.2309.

Synthesis of 4-(2-Amino-4-(*p*-tolyl)pyrimidin-5-yl)-2,6-difluorophenol (54). To 4-chloropyrimidin-2-amine (**22**, 300 mg, 2.32 mmol) in $CHCl_3$ (10 mL) was added NBS (412 mg, 2.32 mmol), and the reaction mixture was stirred overnight at rt. The reaction mixture was partitioned between DCM and water. The organic layer was concentrated. The crude material was triturated with DCM, and the solid was filtered and dried to provide 5-bromo-4-chloropyrimidin-2-amine (300 mg, 62% yield). LCMS (*m*/*z*) 207.9, 209.8, R*t* 0.59 min.

To 5-bromo-4-chloropyrimidin-2-amine (100 mg, 0.48 mmol) and 2,6-difluoro-4-(4,4,5,5-tetramethyl-1,3,2-dioxaborolan-2-yl)phenol **14a** in DME (2 mL) and 2 M sodium carbonate (0.50 mL, 1.00 mmol) was added $PdCl_2$(dppf)·DCM (39.2 mg, 0.05 mmol). The reaction mixture was heated in a microwave at 120 °C for 15 min. The reaction mixture was diluted with ethyl acetate, and the organic layer was separated, dried over sodium sulfate, filtered, and concentrated. The crude material was purified by reverse phase HPLC to obtain 4-(2-amino-4-chloropyrimidin-5-yl)-2,6-difluorophenol (**23**) as a TFA salt (30 mg, 32% yield). LCMS (*m*/*z*) 257.9, 259.9, R*t* 0.56 min.

To 4-(2-amino-4-chloropyrimidin-5-yl)-2,6-difluorophenol (**23**, 30 mg, 0.12 mmol) and *p*-tolylboronic acid (**24**, 19.0 mg, 0.14 mmol) in DME (1 mL) and 2 M sodium carbonate (0.25 mL, 0.50 mmol) was added $PdCl_2$(dppf)·DCM (9.5 mg, 0.01 mmol). The reaction mixture was heated in a microwave at 120 °C for 15 min. The reaction mixture was diluted with ethyl acetate, and the organic layer was separated, dried over sodium sulfate, filtered, and concentrated. The crude material was purified by reverse phase HPLC to obtain **54** as a TFA salt (3.7 mg, 10% yield). ^{1}H NMR (400 MHz, DMSO-d_6) δ 2.14−2.36 (m, 3H), 6.62−6.79 (m, 2H), 6.77−6.95 (m, 2H), 7.00−7.29 (m, 4H), 8.09−8.30 (m, 1H), 10.02−10.22 (m, 1H). LCMS (*m*/*z*) 314.0, R*t* 0.65 min; UPLC 2.31 min. HRMS found *m*/*z* 314.1102; $C_{17}H_{14}N_3OF_2$ requires 314.1105.

Synthesis of 2,6-Difluoro-4-(2-(methylamino)-4-(*p*-tolyl)-pyrimidin-5-yl)phenol (55). To 2,4-dichloropyrimidine (300 mg, 2.01 mmol) and *p*-tolylboronic acid (274 mg, 2.01 mmol) and 2 M sodium carbonate (2.25 mL, 4.50 mmol) in DME (9 mL) was added $PdCl_2$(dppf)·DCM (164 mg, 0.20 mmol). The reaction mixture was heated in a microwave at 120 °C for 15 min. The reaction mixture was

DOI: 10.1021/acs.jmedchem.5b00450
J. Med. Chem. XXXX, XXX, XXX−XXX

partitioned between ethyl acetate and water. The organic layer was separated, dried over sodium sulfate, filtered, and concentrated. The crude material was purified by column chromatography (0−50% EtOAc/heptane) to obtain 2-chloro-4-*p*-tolylpyrimidine (280 mg, 68% yield). LCMS (*m*/*z*) 205.0, 206.9, R*t* 0.98 min.

To 2-chloro-4-*p*-tolylpyrimidine (100 mg, 0.49 mmol) in 2-propanol (2 mL) was added methanamine hydrochloride (39.6 mg, 0.59 mmol) and DIEA (0.26 mL, 1.47 mmol). The reaction mixture was heated in a heating block at 100 °C overnight. The solvent was evaporated, and the crude was purified by column chromatography (0−80% EtOAc/heptane) to provide *N*-methyl-4-*p*-tolylpyrimidin-2-amine as a white solid (80 mg, 78% yield). LCMS (*m*/*z*) 200.0, R*t* 0.60 min.

To *N*-methyl-4-*p*-tolylpyrimidin-2-amine (80 mg, 0.40 mmol) in $CHCl_3$ (4 mL) was added NBS (71.5 mg, 0.40 mmol). The reaction mixture was stirred rt overnight. The reaction mixture was partitioned between DCM and water. The organic layer was separated, dried over sodium sulfate, filtered, and concentrated. The crude material was purified by column chromatography (0−50% EtOAc/heptane) to obtain 5-bromo-*N*-methyl-4-*p*-tolylpyrimidin-2-amine as a white solid (100 mg, 88% yield). LCMS (*m*/*z*) 277.9, 280.0, R*t* 0.95 min.

To 5-bromo-*N*-methyl-4-*p*-tolylpyrimidin-2-amine (50 mg, 0.18 mmol) in DME (2 mL) and 2 M sodium carbonate (0.50 mL, 1.00 mmol) were added 2,6-difluoro-4-(4,4,5,5-tetramethyl-1,3,2-dioxaborolan-2-yl)phenol (69.0 mg, 0.27 mmol) and $PdCl_2$(dppf)·DCM (14.3 mg, 0.02 mmol). The reaction mixture was heated in a microwave at 120 °C for 10 min. The reaction mixture was diluted with ethyl acetate. The organic layer was separated, dried over sodium sulfate, filtered, and concentrated. The crude was purified by reverse phase HPLC to obtain **55** as a TFA salt (35 mg, 58%). ^{1}H NMR (400 MHz, DMSO-d_6) δ 2.27 (s, 3H), 2.85 (s, 3H), 6.74 (d, J = 9 Hz, 2H), 7.05−7.17 (m, 2H), 7.17−7.30 (m, 2H), 8.26 (s, 1H). LCMS (*m*/*z*) 328.0, R*t* 0.73 min, UPLC 2.86 min. HRMS found *m*/*z* 328.1258; $C_{18}H_{16}N_3OF_2$ requires 328.1261.

Synthesis of 2,6-Difluoro-4-(2-(isopropylamino)-4-(*p*-tolyl)-pyrimidin-5-yl)phenol (56). To a mixture of 5-bromo-*N*-isopropyl-4-*p*-tolylpyrimidin-2-amine (40 mg, 0.13 mmol; for synthetic method, see **55**) and 2-(3,5-difluoro-4-methoxyphenyl)-4,4,5,5-tetramethyl-1,3,2-dioxaborolane (**14b**, 35.3 mg, 0.13 mmol; see **50** for synthesis) in DME (2 mL) and 2 M sodium carbonate (0.50 mL, 1.00 mmol) was added $PdCl_2$(dppf)·DCM (10.7 mg, 0.01 mmol). The reaction mixture was heated in a microwave at 120 °C for 15 min. The reaction mixture was diluted with ethyl acetate. The organic layer was separated, dried over sodium sulfate, filtered, and concentrated. The crude residue was taken in DCM (2 mL), and BBr_3 (1 M, 0.65 mL, 0.65 mmol) was added. The reaction was stirred at rt for 4 h. The reaction was diluted with DCM, neutralized with Et_3N (5 equiv), and concentrated. The crude material was purified by reverse phase HPLC to obtain **56** as a TFA salt (18.6 mg, 40% yield). ^{1}H NMR (400 MHz, DMSO-d_6) δ 0.77−1.38 (m, 6H), 2.14−2.37 (m, 3H), 6.69−6.78 (m, 2H), 7.06−7.13 (m, 2H), 7.16−7.28 (m, 2H), 8.04−8.32 (m, 1H), 9.92−10.28 (m, 1H). LCMS (*m*/*z*) 356.2, R*t* 0.84 min; UPLC 3.73 min. HRMS found *m*/*z* 356.1570; $C_{20}H_{20}N_3OF_2$ requires 356.1574.

Synthesis of 2,6-Difluoro-4-(2-(isopropylamino)-4-(4-(4-methylpiperazin-1-yl)phenyl)pyrimidin-5-yl) phenol (57). To 5-bromo-2,4-dichloropyrimidine (100 mg, 0.44 mmol) in DME (3 mL) and 2 M sodium carbonate (0.75 mL, 1.50 mmol) were added 1-methyl-4-(4-(4,4,5,5-tetramethyl-1,3,2-dioxaborolan-2-yl)phenyl)piperazine (133 mg, 0.44 mmol) and $PdCl_2$(dppf)·DCM (35.8 mg, 0.04 mmol). The reaction mixture was stirred at rt overnight. The reaction mixture was diluted with EtOAc and washed with water and sat. NaCl. The organic layer was separated, dried over sodium sulfate, filtered, and concentrated. The crude material was purified by column chromatography (0−10%MeOH/DCM) to provide 5-bromo-2-chloro-4-(4-(4-methylpiperazin-1-yl)phenyl)pyrimidine (30 mg, 20% yield). LCMS (*m*/*z*) 367.0, 368.9, R*t* 0.62 min.

To 5-bromo-2-chloro-4-(4-(4-methylpiperazin-1-yl)phenyl)-pyrimidine (28 mg, 0.08 mmol) in 2-propanol (2 mL) was added propane-2-amine (9.0 mg, 0.15 mmol) and DIEA (0.067 mL, 0.038 mmol). The reaction mixture was heated in a heating block at 110 °C for overnight. The reaction mixture was evaporated on rotovap, and crude 5-bromo-*N*-isopropyl-4-(4-(4-methylpiperazin-1-yl)phenyl)pyrimidin-2-amine was taken to the next step. LCMS (*m*/*z*) 390.2,392.0, R*t* 0.657 min.

To crude 5-bromo-*N*-isopropyl-4-(4-(4-methylpiperazin-1-yl)-phenyl)pyrimidin-2-amine (30 mg, 0.08 mmol) in DME (2 mL) and sodium carbonate (0.50 mL, 1.00 mmol) were added 2-(3,5-difluoro-4-methoxyphenyl)-4,4,5,5-tetramethyl-1,3,2-dioxaborolane (**14b**, 41.5 mg, 0.154 mmol) and $PdCl_2$(dppf)·DCM (6.3 mg, 0.008 mmol). The reaction mixture was heated in a microwave at 120 °C for 10 min. The reaction mixture was diluted with EtOAc. The organic layer was dried over sodium sulfate, filtered, and concentrated to provide crude 5-(3,5-difluoro-4-methoxyphenyl)-*N*-isopropyl-4-(4-(4-methylpiperazin-1-yl)phenyl)pyrimidin-2-amine. LCMS (*m*/*z*) 454.2, R*t* 0.65 min.

The crude material was taken up in DCM (2 mL), and BBr_3 (1.0 M, 0.38 mL, 0.38 mmol) was added. The reaction mixture was stirred at rt for 2 h. The reaction mixture was neutralized with Et_3N and concentrated on rotovap. The crude material was purified by reverse phase HPLC to provide **57** as a TFA salt (6.2 mg, 18% yield). LCMS (*m*/*z*) 440.2, R*t* 0.57 min, UPLC 1.997 min.

Biological Assays. *Inhibition of RSK2 Activity.* Recombinant full-length RSK2 protein (Invitrogen PV4051, Life Technologies, Grand Island, NY) was characterized. RSK2 (0.1 nM) phosphorylates 200 nM peptide substrate (biotin-AGAGRSRHSSYPAGT-OH, biotin-BAD) in the presence of ATP at a concentration equal to the K_m for ATP (20 μM) and appropriate dilutions of RSK inhibitors. The RSK inhibitors were solubilized and diluted in 100% DMSO. The serial dilutions were added to the reaction plate at 0.5 μL/well. To each plate well was added 5 μL of 0.2 nM RSK2 in biochemical assay buffer, 50 mM HEPES, pH 7.5, 10 mM $MgCl_2$, 1 mM DTT, 0.1% BSA fraction V, and 0.01% Tween-20 and incubated for 30 min. The reaction was then started by the addition of 5 μL/well of 40 μM ATP + 400 nM biotin-BAD peptide in biochemical assay buffer. The extent of peptide phosphorylation was detected after 180 min reaction time at room temperature using AlphaScreen technology. The reactions were stopped with 10 μL of 25 mM EDTA + 0.334 nM antiphospho-AKT antibody (CST #9614) + 5 μg/mL of protein A acceptor beads and 5 μg/mL of streptavidin donor beads in 100 mM Tris at pH 7.5, 0.01% Tween-20. The plate was covered with a plate seal, incubated overnight in the dark, then read on an Envision plate reader.

pYB1 Quantification. A quantitative electochemiluminescence (ECL) assay was developed to measure cellular levels of YB1 protein phosphorylated at Ser102. This assay was built using ECL reagents from MesoScale Discovery (MSD, Rockville, MD). Specifically, the cell lysate generated using RIPA lysis buffer (Sigma, R0278−500 mL) was added to unblocked 96-well high bind ECL plates and incubated overnight at 4 °C on a plate shaker. The following day, plates were washed with 1× wash buffer followed by 2 h of rt incubation with 10% BSA diluted in 1× Tris-wash buffer (50 nM Tris at pH 7.5, 0.15 M NaCl, and 0.02% Tween-20). Plates were then washed with 1× wash buffer followed by 2 h of rt incubation with a phospho-specific Ser102 YB1 antibody (Cell Signaling Technologies; C34A2; 1.3 μg/mL). The plates were washed again with 1× wash buffer and then incubated for 2 h at rt with a sulfo-tag goat antirabbit signaling antibody (MSD; 0.5 μg/mL). The plates underwent a final wash before the addition of 1.5× MSD Read buffer and detection of the phospho-YB1 signal in a MSD Sector 6000 plate reader. This assay was routinely run using a mouse BAF cell line engineered to express activated FGFR, but it is readily applicable to other cell lines with sufficient baseline phosphorylation of YB1. Although total YB1 levels were not affected by inhibitor treatment, the phospho-YB1 signal to total YB1 signal was normalized for EC_{50} calculations. The total YB1 was detected through the same protocol described for phospho-YB1 but utilized a total YB1 antibody (Santa Cruz Biotechnology, SC-101198, (59-Q); 1 μg/mL) with a sulfo-tag goat antimouse antibody (MSD; 0.5 μg/mL) for detection.

KinomeScan. Kinase selectivity profiling was carried out by Kinome*Scan* (Ambit/DiscoveRx, Fremont, CA).

DOI: 10.1021/acs.jmedchem.5b00450
J. Med. Chem. XXXX, XXX, XXX−XXX

■ ASSOCIATED CONTENT

Supporting Information

The Supporting Information is available free of charge on the ACS Publications website at DOI: 10.1021/acs.jmedchem.5b00450.

Additional information on the structural biology data collection and refinement statistics (PDF)

■ AUTHOR INFORMATION

Corresponding Author

*Phone: +1 510-879-9421. E-mail: cynthia.shafer@novartis.com.

Author Contributions

†R.J. and M.M. made equal contribution to this work.

Notes

The authors declare no competing financial interest.

■ ACKNOWLEDGMENTS

We thank Weiping Jia for providing the high resolution mass spectroscopy and pK_a data and Elaine Ginn for providing the rat in vitro ADME data highlighted in the manuscript.

■ ABBREVIATIONS USED

EMT, epithelial-mesenchymal transition; HTS, high throughput screening; dppf, 1,1′-bis(diphenylphosphino)ferrocene; dtbpf, 1,1′-bis(di*tert*-butylphosphino)ferrocene; NIS, *N*-iodosuccinimide; DME, 1,2-dimethoxyethane; MW, microwave

■ REFERENCES

(1) Romeo, Y.; Zhang, X.; Roux, P. P. Regulation and function of the RSK family of protein kinases. *Biochem. J.* **2012**, *441*, 553−569.

(2) Lara, R.; Seckl, M. J.; Pardo, O. E. The p90 RSK family meembers: common functions and isoform specificity. *Cancer Res.* **2013**, *73* (17), 5301−8.

(3) Chen, R. H.; Abate, C.; Blenis, J. Phosphorylation of the c-Fos transrepression domain by mitogen-activated protein kinase and 90-kDa ribosomal S6 kinase. *Proc. Natl. Acad. Sci. U. S. A.* **1993**, *90*, 10952−10956.

(4) Shimamura, A.; Ballif, B. A.; Richards, S. A.; Blenis, J. Rsk1 mediates a MEK-MAP kinase cell survival signal. *Curr. Biol.* **2000**, *10* (3), 127−135.

(5) Bonni, A.; Brunet, A.; West, A. E.; Datta, S. R.; Takasu, M. A.; Greenberg, M. E. Cell survival promoted by the Ras-MAPK signaling pathway by transcription-dependent and − independent mechanisms. *Science (Washington, DC, U. S.)* **1999**, *286*, 1358−1362.

(6) Roux, P. P.; Shahbazian, D.; Vu, H.; Holz, M. K.; Cohen, M. S.; Taunton, J.; Sonenberg, N.; Blenis, J. RAS/ERK signaling promotes site-specific ribosomal protein S6 phosphorylation via RSK and stimulates Cap-dependent translation. *J. Biol. Chem.* **2007**, *282* (19), 14056−14064.

(7) Carriere, A.; Cargnello, M.; Julien, L.-A.; Gao, H.; Bonneil, E.; Thibault, P.; Roux, P. P. Oncogenic MAPK signaling stimulates mTORC1 activity by promoting RSK-mediated raptor phosphorylation. *Curr. Biol.* **2008**, *18* (17), 1269−1277.

(8) Doehn, U.; Hauge, C.; Frank, S. R.; Jensen, C. J.; Duda, K.; Nielsen, J. V.; Cohen, M. S.; Johansen, J. V.; Winther, B. R.; Lund, L. R.; Winther, O.; Taunton, J.; Hansen, S. H.; Frodin, M. RSK is a principal effector of the RAS-ERK pathway for eliciting a coordinate promotile/invasive gene program and phenotype in epithelial cells. *Mol. Cell* **2009**, *35*, 511−522.

(9) Stratford, A. L.; Fry, C. J.; Desilets, C.; Davies, A. H.; Cho, Y. Y.; Li, Y.; Dong, Z.; Berquin, I. M.; Roux, P. P.; Dunn, S. E. Y-box binding protein-1 serine 102 is a downstream target of p90 ribosomal S6 kinase in basal-like breast cancer cells. *Breast Cancer Res.* **2008**, *10* (6), R99.

(10) Nguyen, T. L. Targeting RSK: an overview of small molecule inhibitors. *Anti-Cancer Agents Med. Chem.* **2008**, *8* (7), 710−716.

(11) Andreani, A.; Granaiola, M.; Leoni, A.; Locatelli, A.; Morigi, R.; Rambaldi, M.; Varoli, L.; Lannigan, D.; Smith, J.; Scudiero, D.; Kondapaka, S.; Shoemaker, R. H. Imidazo[2,1-b]thiazole guanidinylhydrazones as RSK2 inhibitors. *Eur. J. Med. Chem.* **2011**, *46*, 4311−4323.

(12) Boyer, S. J.; Burke, J.; Guo, X.; Kirrane, T. M.; Snow, R. J.; Zhang, Y.; Sarko, C.; Soleymanzadeh, L.; Swinamer, A.; Westbrook, J.; DiCapua, F.; Padyana, A.; Cogan, D.; Gao, A.; Xiong, Z.; Madwed, J. B.; Kashem, M.; Kugler, S.; O'Neill, M. M. Indole RSK inhibitors. Part 1: Discovery and initial SAR. *Bioorg. Med. Chem. Lett.* **2012**, *22*, 733−737.

(13) Sapkota, G. P.; Cummings, L.; Newell, F. S.; Armstrong, C.; Bain, J.; Frodin, M.; Grauert, M.; Hoffmann, M.; Schnapps, G.; Steegmaier, M. BI-D1870 is a specific inhibitor of the p90 RSK (ribosomal S6 kinase) isoforms *in vitro* and *in vivo*. *Biochem. J.* **2007**, *401*, 29−38.

(14) Roffé, M.; Lupinacci, F. C.; Soares, L. C.; Hajj, G. N.; Martins, V. R. Two widely used RSK inhibitors, BI-D1870 and SL0101, alter mTORC1 signaling in a RSK-independent manner. *Cell. Signalling* **2015**, *27*, 1630−1642.

(15) Cohen, M. S.; Zhang, C.; Shokat, K. M.; Taunton, J. Structural bioinformatics-based design of selective, irreversible kinase inhibitors. *Science (Washington, DC, U. S.)* **2005**, *308*, 1318−1321.

(16) Aronchik, I.; Appleton, B. A.; Basham, S. E.; Crawford, K.; Del Rosario, M.; Doyle, L. V.; Estacio, W. F.; Lan, J.; Lindvall, M. K.; Luu, C. A.; Ornelas, E.; Venetsanakos, E.; Shafer, C. M.; Jefferson, A. B. Novel potent and selective inhibitors of p90 ribosomal S6 kinase reveal the heterogeneity of RSK function in MAPK driven cancers. *Mol. Cancer Res.* **2014**, *12* (5), 803−812.

(17) Miyaura, N.; Suzuki, A. Palladium-catalyzed cross-coupling reactions of organoboron compounds. *Chem. Rev.* **1995**, *95* (7), 2457−2483.

(18) Schindler, T.; Bornmann, W.; Pellicena, P.; Miller, W. T.; Clarkson, B.; Kuriyan, J. Structural mechanism for STI-571 inhibition of Abelson tyrosine kinase. *Science (Washington, DC, U. S.)* **2000**, *289*, 1938−1942.

(19) Cowan-Jacob, S. W.; Fendrich, G.; Floersheimer, A.; Furet, P.; Liebetanz, J.; Rummel, G.; Rheinberger, P.; Centeleghe, M.; Fabbro, D.; Manley, P. W. Structural biology contributions to the discovery of drugs to treat chronic myelogenous leukemia. *Acta Cryst. Acta Crystallogr., Sect. D: Biol. Crystallogr.* **2007**, *63*, 80−93.

(20) Sapkota, G. P.; Cummings, L.; Newell, F. S.; Armstrong, C.; Bain, J.; Morten, F.; Grauert, M.; Hoffmann, M.; Schnapp, G.; Steegmaier, M.; Cohen, P.; Alessi, D. R. BI-D1870 is a specific inhibitor of the p90 RSK (ribosomal S6 kinase) isoforms *in vitro* and *in vivo*. *Biochem. J.* **2007**, *401* (Pt1), 29−38.

(21) Coordinate optimization and relaxed coordinate drive as implemented in Jaguar v. 8.0 from Schrodinger, LLC, New York, NY, 2013, using the B3LYP/6-31G* level of theory with otherwise default settings.

(22) Castro, E. A.; Aliaga, M.; Santos, J. G. Effect of substitution of oxygen by sulfur in the nonleaving group of carbonate: kinetics of the phenolysis and benzenethiolysis of S-methyl aryl thiocarbonates. *J. Phys. Org. Chem.* **2007**, *20*, 533−538.

(23) Unpublished results.

(24) Liu, Y.; Gray, N. S. Rational design of inhibitors that bind to inactive kinase conformations. *Nat. Chem. Biol.* **2006**, *2* (7), 358−364.

(25) Aronov, A. M.; Tang, Q.; Martinez-Botella, G.; Bemis, G. W.; Cao, J.; Chen, G.; Ewing, N. P.; Ford, P. J.; Germann, U. A.; Green, J.; Hale, M. R.; Jacobs, M.; Janetka, J. W.; Maltais, F.; Marland, W.; Namchuk, M. N.; Nanthakumar, S.; Poondru, S.; Straub, J.; ter Haar, E.; Xie, X. Structure-guided design of potent and selective pyrimidylpyrrole inhibitors of extracellular signal-regulated kinase (ERK) using conformational control. *J. Med. Chem.* **2009**, *52*, 6362−6368.

(26) *Molecular Discovery*, 2009 version; Molecular Discovery Ltd.: Middlesex, U.K..

(27) A full listing of the Kinome*Scan* for **46** and **47** is included in the Supporting Information in ref 15. The pan RSK Kinome*Scan* data for **47**

DOI: 10.1021/acs.jmedchem.5b00450
J. Med. Chem. XXXX, XXX, XXX−XXX

are RSK1 0%, RSK2 0%, RSK3 0.05%, and RSK4 0% of control at 10 μM. Kinome*Scan* data are reported as 100-(% control); thus, smaller numbers indicate stronger binders. The information regarding the Kinome*Scan* assays can be found at http://www.discoverx.com/technologies-platforms/competitive-binding-technology/kinomescan-technology-platform/kinomescan-assay-process.

(28) Unpublished data. Compounds **46** and **47** have similar in vitro IC_{50}s against RSK1, 2, and 3.

DOI: 10.1021/acs.jmedchem.5b00450
J. Med. Chem. XXXX, XXX, XXX−XXX